



U.S. Department
of Transportation
**Federal Railroad
Administration**

Investigation on CWR Longitudinal Restraint Behavior in Winter Rail Break and Summer Destressing Operations

Office of Research
and Development
Washington, DC 20590

Research and
Special Programs
Administration
John A. Volpe National
Transportation Systems Center
Cambridge, MA 02142-1093

DOT/FRA/ORD-97/01
DOT-VNTSC-FRA-97-6

Final Report
August 1997

This document is available to the U.S. public through
the National Technical Information Service,
Springfield, VA 22161

NOTICE

This document is disseminated under the sponsorship of the Department of Transportation in the interest of information exchange. The United States Government assumes no liability for its contents or use thereof.

NOTICE

The United States Government does not endorse products or manufacturers. Trade or manufacturers' names appear herein solely because they are considered essential to the objective of this report.

REPORT DOCUMENTATION PAGE

Form Approved
OMB No. 0704-0188

Public reporting burden for this collection of information is estimated to average 1 hour per response, including the time for reviewing instructions, searching existing data sources, gathering and maintaining the data needed, and completing and reviewing the collection of information. Send comments regarding this burden estimate or any other aspect of this collection of information, including suggestions for reducing this burden, to Washington Headquarters Services, Directorate for Information Operations and Reports, 1215 Jefferson Davis Highway, Suite 1204, Arlington, VA 22202-4302, and to the Office of Management and Budget, Paperwork Reduction Project (0704-0188), Washington, DC 20503.

1. AGENCY USE ONLY (Leave blank)		2. REPORT DATE August 1997		3. REPORT TYPE AND DATES COVERED Final Report May 1994 - December 1995	
4. TITLE AND SUBTITLE Investigation on CWR Longitudinal Restraint Behavior in Winter Rail Break and Summer Destressing Operations				5. FUNDING NUMBERS RR719/R7011 DTRS57-93-D-00028	
6. AUTHOR(S) G. Samavedam*, J. Gomes*, A. Kish, A. Sluz					
7. PERFORMING ORGANIZATION NAME(S) AND ADDRESS(ES) Foster-Miller Inc.* 350 Second Ave. Waltham, MA 02154-1196				8. PERFORMING ORGANIZATION REPORT NUMBER DOT-VNTSC-FRA-97-6	
9. SPONSORING/MONITORING AGENCY NAME(S) AND ADDRESS(ES) U.S. Department of Transportation Federal Railroad Administration Office of Research and Development 400 7th St. SW Washington, DC 20590				10. SPONSORING/MONITORING AGENCY REPORT NUMBER DOT/FRA/ORD-97/01	
11. SUPPLEMENTARY NOTES under contract to: U.S. Department of Transportation Research and Special Programs Administration John A. Volpe National Transportation Administration 55 Broadway Cambridge, MA 02142-1093					
12a. DISTRIBUTION/AVAILABILITY STATEMENT This document is available to the public through the National Technical Information Service, Springfield, VA 22161				12b. DISTRIBUTION CODE	
13. ABSTRACT (Maximum 200 words) This report presents the results of investigations on the rail anchor/fastener effects on rail movement and the resulting rail force distribution in continuous welded rail (CWR) track during rail breaks and destressing operations. Two types of tests are used, one for simulating winter rail break and another for destressing operations in summer. The winter rail break test is used to determine the size of the rail gap and the length of the disturbance zone in rail neutral temperature that occur when the rail breaks. The summer rail destressing test is used to determine the deanchored zone length and the rail length to be cut when the rail is destressed. The results are correlated with analyses. The results will be useful to the industry in optimization of their destressing operations. It is shown that the required deanchored section length depends on the precut rail force at the cut location, its distribution along the track and rail longitudinal resistance. By measuring the initial rail force and the resulting gap or longitudinal displacements at the cut locations, the deanchored length can be determined without direct measurement of the initial force distribution and the longitudinal resistance. On the basis of investigations carried out here, improved guidelines are presented for rail gap adjustment in restressing operations using rail heating or hydraulic tensioning.					
14. SUBJECT TERMS continuous welded rail, CWR, neutral temperature, distress, rail anchor, rail break, anchor, fastener				15. NUMBER OF PAGES 72	
				16. PRICE CODE	
17. SECURITY CLASSIFICATION OF REPORT Unclassified	18. SECURITY CLASSIFICATION OF THIS PAGE Unclassified	19. SECURITY CLASSIFICATION OF ABSTRACT Unclassified	20. LIMITATION OF ABSTRACT		

PREFACE

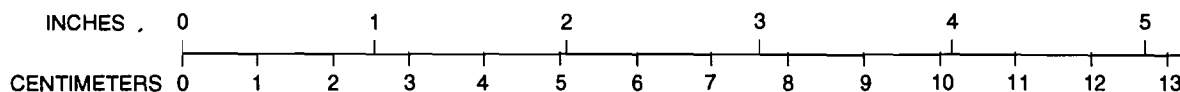
This report describes an investigation of CWR longitudinal restraint behavior in winter rail break and summer destressing operations. This work was jointly performed by Foster-Miller, Inc., on OMNI Contract DTRS-57-93-D-00028, and the John A. Volpe National Transportation Systems Center (Volpe Center). This work was sponsored by the Office of Research and Development of the Federal Railroad Administration (FRA), US Department of Transportation at Washington, DC.

Thanks are due to Mr. Dave Read of the Transportation Technology Center, Pueblo, CO, for his efforts on the test conduct. The authors wish to thank Dr. Herbert Weinstock of the Volpe Center for his valuable technical comments on the draft of this report. Thanks are also due to Mr. Doug Thomson of Foster-Miller for his help in test data compilation and analysis.

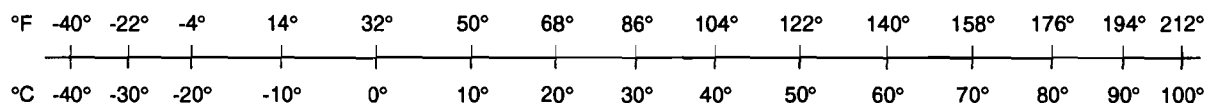
METRIC/ENGLISH CONVERSION FACTORS

ENGLISH TO METRIC	METRIC TO ENGLISH
<p style="text-align: center;">LENGTH (APPROXIMATE)</p> <p>1 inch (in) = 2.5 centimeters (cm) 1 foot (ft) = 30 centimeters (cm) 1 yard (yd) = 0.9 meter (m) 1 mile (mi) = 1.6 kilometers (km)</p>	<p style="text-align: center;">LENGTH (APPROXIMATE)</p> <p>1 millimeter (mm) = 0.04 inch (in) 1 centimeter (cm) = 0.4 inch (in) 1 meter (m) = 3.3 feet (ft) 1 meter (m) = 1.1 yards (yd) 1 kilometer (km) = 0.6 mile (mi)</p>
<p style="text-align: center;">AREA (APPROXIMATE)</p> <p>1 square inch (sq in, in²) = 6.5 square centimeters (cm²) 1 square foot (sq ft, ft²) = 0.09 square meter (m²) 1 square yard (sq yd, yd²) = 0.8 square meter (m²) 1 square mile (sq mi, mi²) = 2.6 square kilometers (km²) 1 acre = 0.4 hectare (ha) = 4,000 square meters (m²)</p>	<p style="text-align: center;">AREA (APPROXIMATE)</p> <p>1 square centimeter (cm²) = 0.16 square inch (sq in, in²) 1 square meter (m²) = 1.2 square yards (sq yd, yd²) 1 square kilometer (km²) = 0.4 square mile (sq mi, mi²) 10,000 square meters (m²) = 1 hectare (ha) = 2.5 acres</p>
<p style="text-align: center;">MASS - WEIGHT (APPROXIMATE)</p> <p>1 ounce (oz) = 28 grams (gm) 1 pound (lb) = .45 kilogram (kg) 1 short ton = 2,000 pounds (lb) = 0.9 tonne (t)</p>	<p style="text-align: center;">MASS - WEIGHT (APPROXIMATE)</p> <p>1 gram (gm) = 0.036 ounce (oz) 1 kilogram (kg) = 2.2 pounds (lb) 1 tonne (t) = 1,000 kilograms (kg) = 1.1 short tons</p>
<p style="text-align: center;">VOLUME (APPROXIMATE)</p> <p>1 teaspoon (tsp) = 5 milliliters (ml) 1 tablespoon (tbsp) = 15 milliliters (ml) 1 fluid ounce (fl oz) = 30 milliliters (ml) 1 cup (c) = 0.24 liter (l) 1 pint (pt) = 0.47 liter (l) 1 quart (qt) = 0.96 liter (l) 1 gallon (gal) = 3.8 liters (l) 1 cubic foot (cu ft, ft³) = 0.03 cubic meter (m³) 1 cubic yard (cu yd, yd³) = 0.76 cubic meter (m³)</p>	<p style="text-align: center;">VOLUME (APPROXIMATE)</p> <p>1 milliliter (ml) = 0.03 fluid ounce (fl oz) 1 liter (l) = 2.1 pints (pt) 1 liter (l) = 1.06 quarts (qt) 1 liter (l) = 0.26 gallon (gal) 1 cubic meter (m³) = 36 cubic feet (cu ft, ft³) 1 cubic meter (m³) = 1.3 cubic yards (cu yd, yd³)</p>
<p style="text-align: center;">TEMPERATURE (EXACT)</p> <p style="text-align: center;">$^{\circ}\text{C} = 5/9(^{\circ}\text{F} - 32)$</p>	<p style="text-align: center;">TEMPERATURE (EXACT)</p> <p style="text-align: center;">$^{\circ}\text{F} = 9/5(^{\circ}\text{C}) + 32$</p>

QUICK INCH-CENTIMETER LENGTH CONVERSION



QUICK FAHRENHEIT-CELSIUS TEMPERATURE CONVERSION



For more exact and or other conversion factors, see NIST Miscellaneous Publication 286, Units of Weights and Measures. Price \$2.50. SD Catalog No. C13 10286.

Updated 8/1/96

TABLE OF CONTENTS

<u>Section</u>	<u>Page</u>
1. INTRODUCTION	1
1.1 Maintenance Practice	1
1.2 Research Need	1
1.3 Technical Discussion	2
1.4 Objectives	3
1.5 Accomplishments	4
2. RAIL DESTRESSING MODEL	5
2.1 Theoretical Model	6
2.2 Experimental Correlations	12
3. WINTER RAIL BREAK INVESTIGATIONS	13
3.1 Test Setup	13
3.2 Test Conduct	14
3.3 WRB Test Data and Analysis	15
3.3.1 Test Data	15
3.3.2 Analysis	16
3.3.3 Key Findings	25
4. SUMMER RAIL DESTRESSING INVESTIGATIONS	26
4.1 Test Setup	26
4.2 Test Conduct	27
4.3 SRD Test Data and Analysis	27
4.3.1 Test Data	27
4.3.2 Analysis	29
4.3.3 Key Findings	38
5. IMPROVED GUIDELINES FOR RAIL DESTRESSING	40
5.1 Selection of Deanchored Section Length	40
5.2 Gap Adjustment for Restressing under Rail Heating	41
5.2.1 Artificial Heating	41
5.2.2 Solar Heating	41
5.3 Gap Adjustment under Hydraulic Tensioning	43

TABLE OF CONTENTS (cont.)

<u>Section</u>	<u>Page</u>
6. CONCLUSIONS AND RECOMMENDATIONS	46
6.1 Conclusions	46
6.2 Recommendations	47
APPENDIX - INITIAL RAIL FORCE DISTRIBUTIONS - LINEAR FITS	A-1
REFERENCES	R-1

LIST OF ILLUSTRATIONS

<u>Figure</u>	<u>Page</u>
1-1. Definition of Local Region and Distressed Rail Length	2
2-1. Rail Motion and Rotation of Ties	5
2-2. Longitudinal Resistance Characteristic	6
2-3. Force and Displacement Definitions	7
2-4. Anticipated Force and Displacement Distributions	8
3-1. Instrumentation Deployment	13
3-2. Definition and Measurement of Rail Gap.....	15
3-3. WRB1 Rail Force Data	17
3-4. WRB2 Rail Force Data	17
3-5. WRB1 Rail Force Change Due to Cut.....	18
3-6. WRB1 Rail Displacement Due to Cut	19
3-7. WRB2 Rail Force Change Due to Cut.....	19
3-8. WRB2 Rail Displacement Due to Cut	20
3-9. WRB3 Rail Force Change Due to Cut.....	20
3-10. WRB3 Rail Displacement Due to Cut	21
3-11. WRB4 Rail Force Change Due to Cut.....	21
3-12. WRB4 Rail Displacement Due to Cut	22
3-13. WRB5a Rail Force Change Due to Cut (ETA)	22
3-14. WRB5a Rail Displacement Due to Cut (ETA)	23
3-15. WRB5b Rail Force Change Due to Cut (EOTA)	23
3-16. WRB5b Rail Displacement Due to Cut (EOTA)	24
4-1. Definition and Measurement of Cutout Length and Rail Gap.....	28
4-2. SRD1 Rail Force Change Due to Cut	30
4-3. SRD1 Rail Displacement Due to Cut	31
4-4. SRD2 Rail Force Change Due to Cut	31
4-5. SRD2 Rail Displacement Due to Cut	32
4-6. SRD3 Rail Force Change Due to Cut	32
4-7. SRD3 Rail Displacement Due to Cut	33
4-8. SRD4 Rail Force Change Due to Cut	33
4-9. SRD4 Rail Displacement Due to Cut	34
4-10. SRD5a Rail Force Change Due to Cut	34
4-11. SRD5a Rail Displacement Due to Cut	35
4-12. SRD5b Rail Force Change Due to Cut	35
4-13. SRD5b Rail Displacement Due to Cut	36
4-14. SRD6 Rail Force Change Due to Cut	36
4-15. SRD6 Rail Displacement Due to Cut	37
4-16. SRD7 Rail Force Change Due to Cut	37
4-17. SRD7 Rail Displacement Due to Cut	38
5-1. End Movement in Solar Heating Method of Restressing	42
5-2. End Movement in Hydraulic Expander Method of Restressing	44

LIST OF TABLES

<u>Table</u>		<u>Page</u>
3-1.	Winter Rail Break Test Matrix	14
3-2.	Test Data	16
3-3.	Analysis Predictions	18
4-1.	Summer Rail Destressing Test Matrix	26
4-2.	Test Data	29
4-3.	Analysis Predictions	30

LIST OF SYMBOLS

A	Rail cross-sectional area
E	Young's Modulus
f_0	Longitudinal resistance per unit length
k_f	Linear slope of longitudinal resistance
L	Length of deanchored zone on either side-of rail cut
L_d	Calculated length of deanchored zone
P_0	Initial rail force at center of disturbed zone
P_i	Rail force distribution prior to cut
P_f	Rail force distribution following cut
T_N	Initial rail neutral temperature
T_R	Rail temperature
ΔT	Rail temperature increase
u	Longitudinal displacement of rail
u_0	Longitudinal displacement of rail at cut location
x	Coordinate along length of rail
α	Coefficient of thermal expansion

EXECUTIVE SUMMARY

This report deals with the problem of destressing continuous welded rails (CWR) and adjustment of the rail gap prior to rewelding for setting up of desired neutral temperature.

Destressing CWR in summer conditions when high compressive loads can exist in the rails prone to buckling, involves rail cutting to relieve the load, removal of anchors over some length (deanchored length) and setting up an accurate rail gap for rewelding at the desired neutral temperature. If the rail temperature is lower than the neutral temperature, rail heating or restressing with hydraulic tensors may also be required prior to rewelding. In this report, a rational theory has been developed to provide guidelines for destressing and rewelding CWR tracks in summer conditions. The theory is also applicable for winter conditions, which can result in tensile fractures. The rail gap due to fracture can be calculated using the theory.

To validate the proposed theory, tests simulating summer and winter conditions were performed at the Transportation Technology Center, Pueblo, CO. Required rail thermal loads were obtained by appropriate initial neutral temperature settings (low for summer destressing tests and high for winter rail break simulations) and also by letting rails reach appropriate temperatures under diurnal solar heating, prior to rail cutting operations. Thus high afternoon rail temperature gave high compressive loads for summer simulations and low temperatures at dawn produced large tensile loads for winter tests.

The test sections were fully instrumented with strain gauges for rail force, thermocouples for rail temperatures and with displacement transducers for rail longitudinal movements. Rail gap sizes after rail cutting were also measured. Force distributions before and after rail cutting as well as after rail anchor removal were recorded. Rail anchors were removed over sections with locked up loads of no more than 20 kips in many tests. Reasonable correlations were found between the theoretical predictions and experimental data. Based on this work, the following conclusions are drawn:

1. The theoretical analysis based on constant longitudinal resistance provides computationally simple expressions for force and displacement distributions and for determining the deanchored section lengths and required rail gap prior to rewelding. The theory also assumes that precut rail force distribution is linear along the track. The theory appears to be adequate for practical applications.
2. The deanchored section length for complete destressing is influenced by 1) initial rail force at the cut location, 2) the overall force distribution along the track and 3) the rail longitudinal resistance (offered by rail anchors/ballast). Other parameters remaining constant, the deanchored length increases with the initial rail force and decreases with increasing longitudinal resistance.

3. The longitudinal resistance of track tested with every tie anchored (ETA) is almost twice that with every other tie anchored (EOTA). For uniform initial rail force distribution, the required deanchored section lengths are also in the same proportion.
4. The theory shows that the rail gap size to be adjusted prior to the application of tensors is more than commonly recommended in the industry practice. This is due to the additional rail movement, caused by the deanchored section under applied tensile load. Significant errors on the nonconservative side can occur, if this movement is not accounted for in the gap, particularly when the track is weak longitudinally and high neutral temperature is desired.

1. INTRODUCTION

One of the key parameters influencing the safety of continuous welded rail track (CWR) is the rail neutral temperature. If the neutral temperature is too high, large tensile forces can be generated in winter, causing tensile fracture in the presence of rail defects. If the neutral temperature is too low, large compressive rail stresses will be developed in summer causing lateral buckling in the presence of initial track misalignments and vehicle loads.

1.1 MAINTENANCE PRACTICE

Currently, if a rail break occurs in winter, the track crew can use a temporary bolted joint or decide to weld and set the correct neutral temperature in the rail. Because the rail temperatures tend to be lower than the required neutral temperature (80° to 110°F), the rail has to be *restressed* by means of hydraulic pullers prior to welding to set the equivalent neutral temperature. In some situations artificial or natural solar rail heating may be employed instead of hydraulic pullers to achieve neutral temperature. If a bolted joint is used in winter, it will be replaced by welding at the desired neutral temperature in early spring.

Conversely, in late spring and summer, CWR may be intentionally cut by the track crew at locations where the rail may exhibit excessive compressive loads in the form of its “tightness” in tie plates or small sun kinks. Rail cutting relieves the rail force at the cut location and removal of rail anchors over a section of rail will *destress* the rail. The rail cutting is typically done on a hot day, when a large compressive load exists in the rail. After rail cutting and destressing, the rail is reanchored and welded when the rail temperature is still high and close to the desired neutral temperature.

1.2 RESEARCH NEED

There are two basic issues which need to be addressed in rail destressing and restressing in winter and summer conditions:

1. Determination of deanchored rail segment length.
2. Adjustment of rail gap prior to welding.

In addressing these issues, it will be assumed that the large tensile loads in winter prior to rail break and the large compressive load in summer prior to rail cutting are confined to a local region at the rail break or cut. At some distance away from the break or cut, the rail force is at its normal level depending on the temperature. Thus at some distance away, the rail neutral temperature remains at its correct value.

When the rail breaks or is cut, the rail force change may be experienced over a large distance although the initial rail force variation is confined to a small zone prior to cut. This is

schematically shown in Figure 1-1. In order to set the CWR to its “original” uniform condition, it is necessary to distress (remove anchors) the rail over the length $2L_d$ as shown in the figure.

The adjustment of the rail “expansion” gap prior to welding is required for the following reasons. This gap should accommodate weld (typically between 0.75 to 1 in.) and any expansion or contraction of the deanchored halves of the rail section due to temperature changes prior to welding. If restressing is to be performed using a hydraulic puller, the initial gap should accommodate an appropriate rail longitudinal movement to give the desired rail force (equivalent to the required neutral temperature) prior to welding.

1.3 TECHNICAL DISCUSSION

At present there are no rational guidelines on the rail length to be distressed and the rail gap to be adjusted for obtaining desired CWR neutral temperatures. Clearly, the deanchored length and rail gap will depend on the following parameters:

1. The initial rail force prior to rail fracture or cut.
2. The combined longitudinal resistance offered by anchors preventing longitudinal rail movement with respect to ties, and by the ballast preventing tie longitudinal movement.
3. Rail size.

If these parameters are known, the rail gap, the resulting rail force distribution after the cut, and the required deanchored track length can be calculated. The basis of these calculations will be the differential equations of equilibrium governing longitudinal forces and displacements. The two parameters (a) and (b) are seldom known in advance, and may vary from location to location in the field conditions. The longitudinal resistance is particularly a difficult parameter

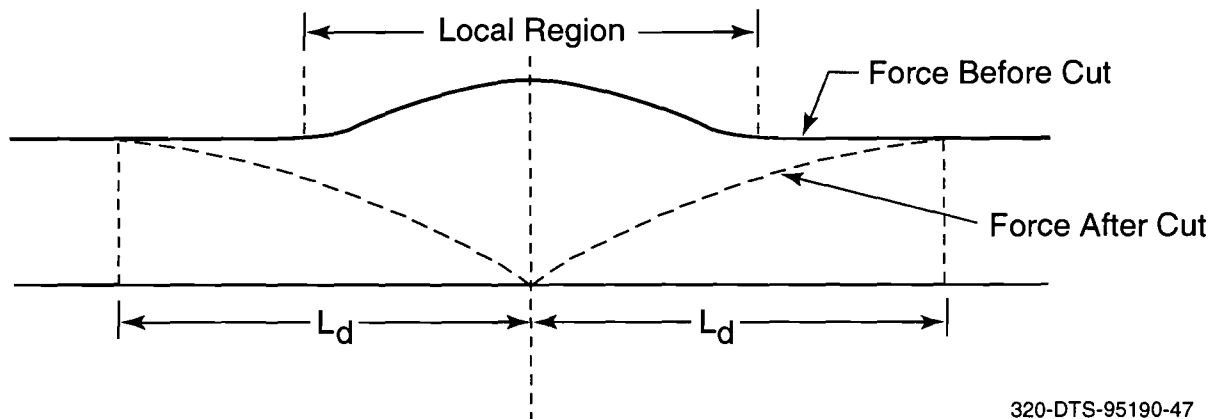


Figure 1-1. Definition of Local Region and Distressed Rail Length

to evaluate since it may be governed by rail slipping through anchors at some location, and ties moving in the ballast at some other locations. It is not practical to measure the longitudinal resistance at a large number of locations. Many measurements are required to obtain a statistically reliable average resistance over several hundred feet of track that is typically involved in the destressing operations in a single rail cut. Consequently, indirect means will be needed to quantify this parameter for use in theoretical predictions and practice.

In this work, a theoretical analysis is developed based on the assumption that the rail longitudinal resistance is constant. This is justified since the expected longitudinal displacement near cut locations is large and sliding friction between the rail and its anchors may also be a major contributor to the overall longitudinal resistance. As shown later, constant resistance idealization produces simple expressions for the rail response, which seem to correlate satisfactorily with the test data. Linear resistance assumption was also tried in the analysis, but abandoned as it did not produce good correlations. More rigorous nonlinear idealizations for the resistance resulted in unwieldy analysis and was not pursued.

The proposed methodology is validated here by correlating theoretical results with the rail force and the longitudinal displacement distributions measured on a fully instrumented test track on which both Winter Rail Break and Summer Destressing operations were simulated.

1.4 OBJECTIVES

The overall objective of the work is to develop a field applicable methodology for optimum destressing and restressing of CWR in winter and summer conditions. The specific objectives pursued here are:

1. Develop a rational and practical approach for evaluation of the rail force and the rail longitudinal displacement distribution, when the rail is cut.
2. Evaluate the required deanchored length for optimum destressing and the final gap for restressing and rewelding at the desired neutral temperature.
3. Simulate Winter Rail Break (WRB) and Summer Rail Destressing (SRD) operations for ETA and EOTA patterns on an instrumented test track, and validate the theoretical approach in (1). Correlate the calculated deanchored length from (2) with the results derived from the rail force test data.
4. Compare the theoretical results on the gap size required under rail heating or hydraulic rail pullers (when restressing the rail for a neutral temperature higher than the rail temperature) with the current railroad practices and propose improved guidelines for the industry in their restressing operations.

1.5 ACCOMPLISHMENTS

In this project, investigations were carried out for the CWR analysis of the conditions described above. The WRB test provided the data on rail movements, rail gap size, and redistribution of rail force and neutral temperature that occur when the rail fractures in winter. The SRD test provided the data used to calculate the rail deanchored zone length and steel to be cut out when destressing the rail during summer conditions. A model was also used in this project to determine the effectiveness and influence of the rail anchors on the rail movements and neutral temperatures. The results of the model and tests show that the disturbance zone in CWR due to the rail break at high tensile load can extend to several hundred feet on either side of the rail break. To restress the rail to a uniform neutral temperature, it appears necessary to deanchor over this long disturbance zone. The disturbance zone is shorter if every tie is anchored, which is advantageous over the every other tie anchored scenario that is currently used in most applications.

After validating the theory on the basis of experimental data, the theoretical data have been extended to size the required expansion gap for restressing CWR under rail heating or hydraulic tensioning. The required gap is found to be larger than typically used by the industry, which indicates nonconservative results in the industry practice. Therefore, improved guidelines on rail restressing are included in this report.

2. RAIL DESTRESSING MODEL

A fundamental parameter in the studies concerning the Winter Rail Break and the Summer Destressing Operations is the longitudinal resistance experienced by a single rail after it is cut and its initial thermal load is released at the cut location. The resistance is a complex combination of the anchors and the ballast. The other rail can generally be assumed to be intact with no longitudinal motion. As shown in Figure 2-1, the longitudinal motion of the cut rail may tend to move the anchored ties. Since the ties are effectively 'pinned' at one end by the uncut rail, the ties may tend to rotate in the lateral plane, thus affecting the apparent resistance to the cut rail.

The longitudinal motion of the cut rail is resisted by the fasteners, ties and ballast. (Note that this "single rail longitudinal resistance" differs from the "track longitudinal resistance" encountered in CWR track buckling (1), which considers the longitudinal motion of both rails.) The resistance is a combination of the individual resistances offered by fasteners and ballast via the ties. In principle, the two components of the resistance can be considered as two "springs" in series. Thus, the fastener spring resistance can be determined (as is typically done in the laboratory using the so-called "pull" tests) by holding the ties rigidly and pulling the rail longitudinally. The tie-ballast resistance can be evaluated in the field condition by mobilizing the ties longitudinally. Tests of this type were performed at the Transportation Technology Center, Pueblo, CO as a part of the program presented here. These tests will be described in a future report. Significant variation between ties was found in these test data which was attributed to the construction and maintenance of the track. A large number of tests would be required to obtain a reliable statistical average of the resistance.

It appears that a simple and convenient way of determining the effective resistance of the single rail is to use a semi-infinite single rail longitudinally loaded at the free end and determine the resulting end displacement. From the load-displacement characteristic, the longitudinal stiffness or resistance can be back-calculated. The resulting resistance will be clearly a more

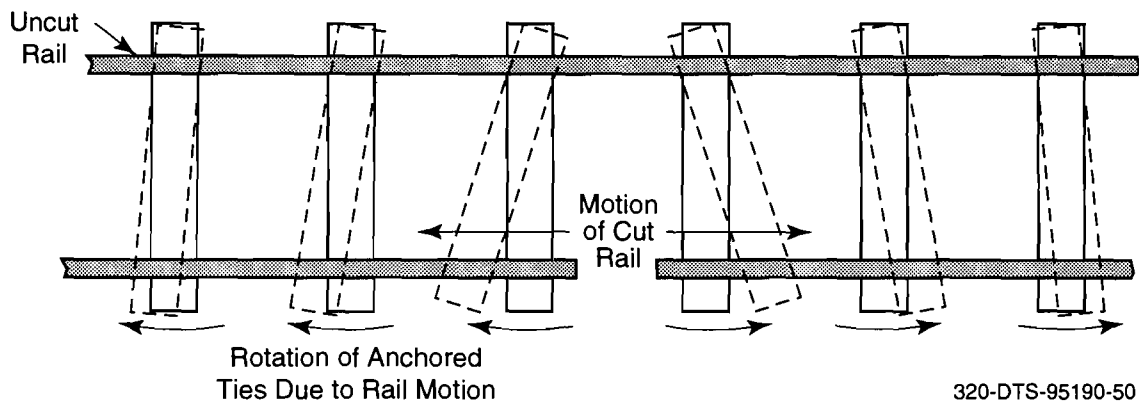


Figure 2-1. Rail Motion and Rotation of Ties

reliable average for the entire semi-infinite section than the value determined from tests on a few selected ties/fasteners. In fact, in the present work, the Summer Destressing and Winter Rail Break tests closely resemble that of the loaded semi-infinite rail, since the initial load already exists in the rail prior to cut. Thus, the test data can be directly used to determine the longitudinal resistance from fasteners and ballast.

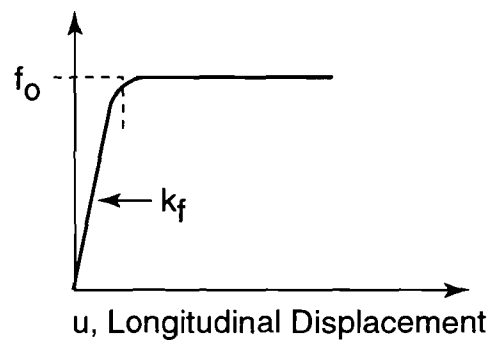
2.1 THEORETICAL MODEL

The investigations on the rail longitudinal behavior in Summer Destressing and Winter Rail Break scenarios will be made under the assumption that the longitudinal resistance characteristic is constant. Such an assumption has been made in an earlier theoretical analysis (2) of these problems. This work produced reasonable results on the rail gap and the required deanchored lengths of CWR, which are consistent with some previous field data. However, this work did not deal with the problem of determining the rail longitudinal resistance which is site specific to these operations. Also, the work did not address the problem of restressing the CWR by rail heating or hydraulic tensioning.

Alternate assumptions such as a bilinear longitudinal resistance (Figure 2-2) may also be applicable. If a bilinear idealization is considered for the resistance, the problem is greatly complicated by the need for more than parameter in the resistance characterization, and the resulting analysis.

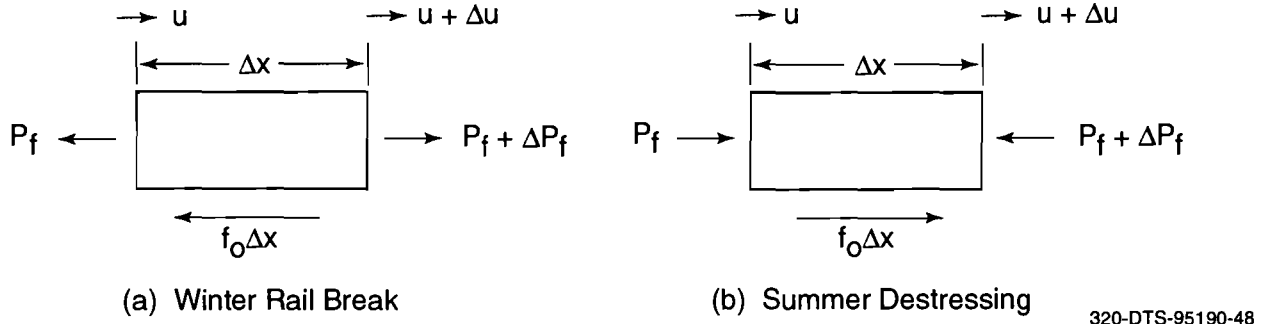
Figure 2-3 shows the forces at equilibrium on the rail element. A differential force ΔP_f across a rail length of Δx will produce a net longitudinal displacement of Δu on the rail element. The combined resistance generated by the fastener and the ballast will be assumed constant for a given track, and the constant will be represented by f_0 , which is called the longitudinal resistance.

The following section derives the relationships between the rail force, rail displacement or gap after rail cut, and the rail longitudinal resistance. These are useful in determining the required deanchored length and in an assessment of the overall CWR longitudinal behavior.



320-DTS-95190-49

Figure 2-2. Longitudinal Resistance Characteristic



320-DTS-95190-48

Figure 2-3. Force and Displacement Definitions

The change in rail force (ΔP) due to the rail cut is shown in Figure 2-4 where P_i is the initial rail force distribution and P_f is the final rail force distribution after the cut. To properly evaluate the data presented in Sections 3 and 4, the nonuniform initial force distribution must be taken into account (due to difficulties in establishing a constant initial force in the tests). As in Figure 2-3, u is the displacement in the longitudinal direction (x -direction). For the WRB, the displacement can be determined from the integral equation

$$u = \int_x^{L_d} (P_i - P_f) / AE dx \quad (2-1)$$

where P_i and P_f are considered to be positive and functions of x . It is assumed that at some distance, L_d , the force change and displacement are zero. Since the rail has moved after the cut, longitudinal resistance will be generated in the anchors. The configuration of the rail is determined by the final residual force equilibrium (Figure 2-3)

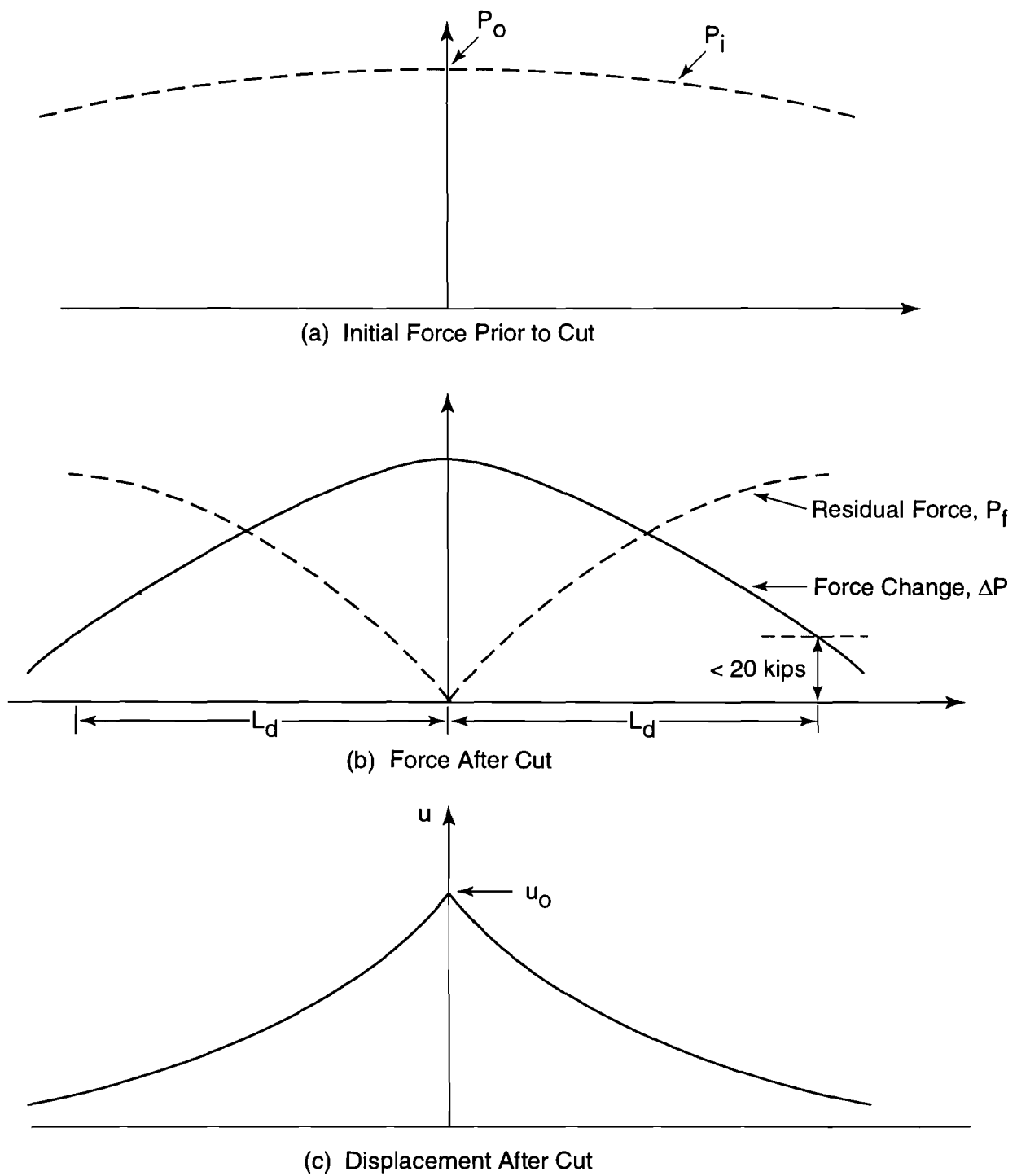
$$\frac{dP_f}{dx} = f_0 \quad (2-2)$$

Differentiating both sides of Equation (2-1) with respect to x and after rearranging, one finds that

$$P_f = P_i + AE \frac{du}{dx} \quad (2-3)$$

Substitution of Equation (2-3) into (2-2) gives

$$\frac{d^2u}{dx^2} = -\frac{1}{AE} \left(\frac{dP_i}{dx} - f_0 \right) \quad (2-4)$$



320-DTS-95190-51

Figure 2-4. Anticipated Force and Displacement Distributions

Equation (2-4) shows that the longitudinal displacement depends on the initial force distribution. This distribution will be assumed as

$$P_i = P_0 - \lambda x \quad (2-5)$$

The linearly varying P_i is adequate for most cases. λ can be negative which represents increasing rail force from the cut location. The left and right sides of the cut location may also exhibit different values of λ . From Equations (2-4) and (2-5)

$$\frac{d^2 u}{dx^2} = \frac{\lambda + f_0}{AE} \quad (2-6)$$

The solution of the differential equation can be expressed as

$$u = \frac{(\lambda + f_0)}{AE} \frac{x^2}{2} + C_1 x + C_2 \quad (2-7)$$

The boundary conditions are

At $x = 0$,

$$u = u_0 \text{ (measured)} \quad (2-8.1)$$

$$AE \frac{du}{dx} = -P_0 \text{ (measured)} \quad (2-8.2)$$

At $x = L_d$,

$$u = 0 \text{ (zero displacement)} \quad (2-8.3)$$

$$\frac{du}{dx} = 0 \text{ (zero force change)} \quad (2-8.4)$$

Here both u_0 and P_0 are considered to be positive.

The four conditions 2-8.1 to 2-8.4 determine the four unknowns, C_1 , C_2 , L_d and f_0 . It can be shown that

$$C_1 = -\frac{P_0}{AE} \quad (2-9.1)$$

$$C_2 = u_0 \quad (2-9.2)$$

$$L_d = \frac{2u_0AE}{P_0} \quad (2-9.3)$$

$$f_0 = \frac{P_0^2}{2u_0AE} - \lambda \quad (2-9.4)$$

Equations (2-9.3) and (2-9.4) are the required equations. The final equations for u and ΔP are

$$u = \frac{P_0}{AE} \left(\frac{x^2}{2L_d} - x \right) + u_0 \quad (2-10.1)$$

$$\Delta P = P_0 \left(1 - \frac{x}{L_d} \right) \quad (2-10.2)$$

For the Summer Destressing operation, the analysis can be carried out in a similar fashion. Representing the rail compressive forces before and after cutting by P_i and P_f (which are also considered positive here with no sign difference) the displacement is given by

$$u = \int_x^{L_d} (P_i - P_f) / AE \, dx \quad (2-11)$$

where u is considered positive in the positive x direction. The differential equation for u can be shown as

$$\frac{d^2u}{dx^2} = \frac{-(\lambda + f_0)}{AE} \quad (2-12)$$

The solution of the differential equation can be expressed as

$$u = -\frac{(\lambda + f_0)}{AE} \frac{x^2}{2} + C_1x + C_2 \quad (2-13)$$

The boundary conditions are

At $x = 0$,

$$u = -u_0 \text{ (measured, absolute value)} \quad (2-14.1)$$

$$AE \frac{du}{dx} = P_0 \text{ (measured, absolute value)}$$

At $x = L_d$,

$$u = 0 \tag{2-14.3}$$

$$\frac{du}{dx} = 0 \tag{2-14.4}$$

These equations give

$$C_1 = \frac{P_0}{AE} \tag{2-15.1}$$

$$C_2 = -u_0 \tag{2-15.2}$$

and exactly the same expressions for L_d and f_0 as in the case of Winter Rail Break model. Thus Equations (2-9.3) and (2-9.4) are applicable for both Winter Rail Break and Summer Destressing operations. In these equations u_0 and P_0 are absolute quantities with no sign convention. It can be shown that the expression for u for Summer Destressing is

$$u = - \left\{ \frac{P_0}{AE} \left(\frac{x^2}{2L_d} - x \right) + u_0 \right\} \tag{2-15.3}$$

The expression for ΔP is as before

$$\Delta P = P_0 \left(1 - \frac{x}{L_d} \right) \tag{2-15.4}$$

The fact that Equation (2-9.3) for the deanchored section length, L_d , is independent of λ is a great advantage since the initial force *distribution* is not necessary in the calculation. However λ will be needed if it is desired to evaluate the longitudinal resistance, f_0 . Although λ does not explicitly appear in Equation (2-9.3), it has a significant influence on u_0 and hence L_d indirectly. In practical applications it will be adequate to measure only u_0 and P_0 for determination of L_d . The displacement u_0 can be shown as

$$u_0 = \frac{P_0^2}{2(f_0 + \lambda)AE} \tag{2-16}$$

This equation will be helpful in the development of improved guidelines discussed in Section 5.

It may be noted that the combined assumptions of a linearly varying P_i and a constant longitudinal resistance resulted in a linearly varying strain along the rail, hence the deanchoring length may be approximated by dividing the measured displacement at the cut, u_0 , by the *average* strain along the deanchoring length ($P_0/2AE$) as implied by equation (2-9.3).

Required Deanchored Length

The required deanchoring length is clearly at least L_d , since this is the length of disturbance zone due to the rail cut. Beyond this length, the rail force is unaltered and need not be adjusted, unless the initial neutral temperature beyond L_d also is low. Rail cutting and removing anchors up to L_d on either side of the cut will be called “local” destressing as opposed to “global” destressing which may extend removal of anchors far beyond L_d .

Clearly, the rail force change, $\Delta P (P_i - P_f)$ as well as the longitudinal displacement at and beyond L_d is zero. In practice $\Delta P \leq 20$ kips may be considered adequate for determining L_d although in this work $\Delta P = 0$ is used for evaluation of theoretical results. Due to the initial linear part of the longitudinal resistance (Figure 2-2), the force decay occurs more slowly beyond L_d and does not fall to zero. However, the error due to neglecting the linear part is considered to be small for the investigations presented here.

If the longitudinal resistances on the two sides of the cut location are not equal (e.g., at the bridge entrance or exit, near switches) then the displacements of the two halves of the rail will be different. Equations (2-9.3) and (2-9.4) can be used for the two halves separately.

2.2 EXPERIMENTAL CORRELATIONS

The test data will be correlated with the theoretical analysis presented in subsection 2.1. From the measured initial force, P_0 and the displacement, u_0 at the cut location, L_d and f_0 will be evaluated using Equations (2-9.3) and (2-9.4). The longitudinal displacement and the change in the rail force will be evaluated using the Equations (2-10.1) and (2-10.2), respectively.

The anticipated distributions for displacement and drop in the rail force are shown in Figure 2-4. These will be correlated with the experimental data collected using the displacement transducers and strain gauges. The deanchored length determined from (2-9.3) will also be correlated with the test data in the rail force as obtained from the strain gauge output.

3. WINTER RAIL BREAK INVESTIGATIONS

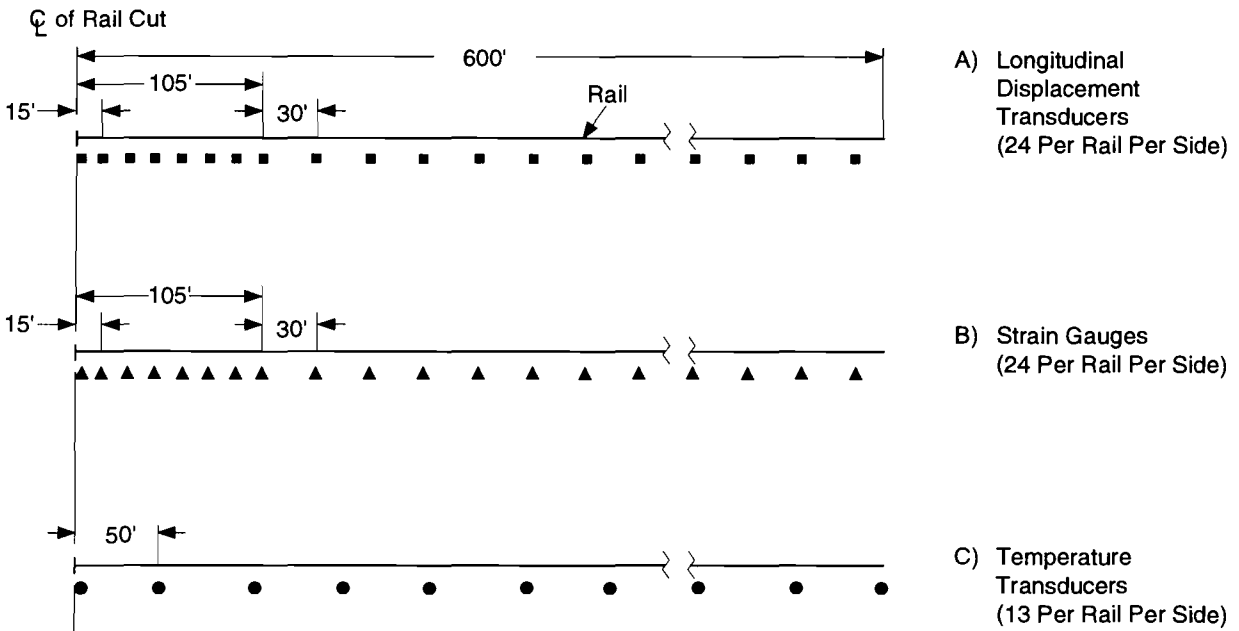
The test conduct and test measurements are briefly described here, followed by a test data summary and analytic correlations.

3.1 TEST SETUP

The tests were conducted on a 1200 ft long CWR tangent track section in the balloon loop at the Transportation Technology Center, Pueblo, CO. The rails were 136#RE. Wood ties with snap-on channel anchors were used. The ballast material was slag.

The rails were instrumented with strain gauges to give rail force, with linear potentiometers for rail and tie longitudinal displacements, and with thermocouples for rail temperature. The instrumentation deployment was as in Figure 3-1. The transducers were placed at closer intervals in the central zone for more accurate assessment of the rail longitudinal behavior near the cut location. A digital data acquisition system with display of the transducer output on the monitor screen was employed.

The test matrix shown in Table 3-1 consists of five tests. The first four tests simulated the EOTA pattern on the test rail. The anchoring pattern on the other rail was also EOTA except in test No. 4, in which every tie was anchored. (The ETA condition in test No. 4 was required for the Summer Destressing test that was subsequently performed on this rail.)



191-DTS-9718-3

Figure 3-1. Instrumentation Deployment

Table 3-1. Winter Rail Break Test Matrix

Test No.	Anchor Pattern		Approximate T_N at Center (°F)	Approximate Rail Cut Temperature, T_C (°F)		Comment
	Test Rail	Other Rail				
1	EOTA	EOTA	80	<10	{	Basic tests at high tensile force
2	EOTA	EOTA	80	<10		
3	EOTA	EOTA	100	60	{	Tests at moderate force levels
4	EOTA	ETA	120	60		
5a	ETA	ETA	>100	50	{	Provide direct comparison of EOTA versus ETA
5b	EOTA	EOTA	>100	50		

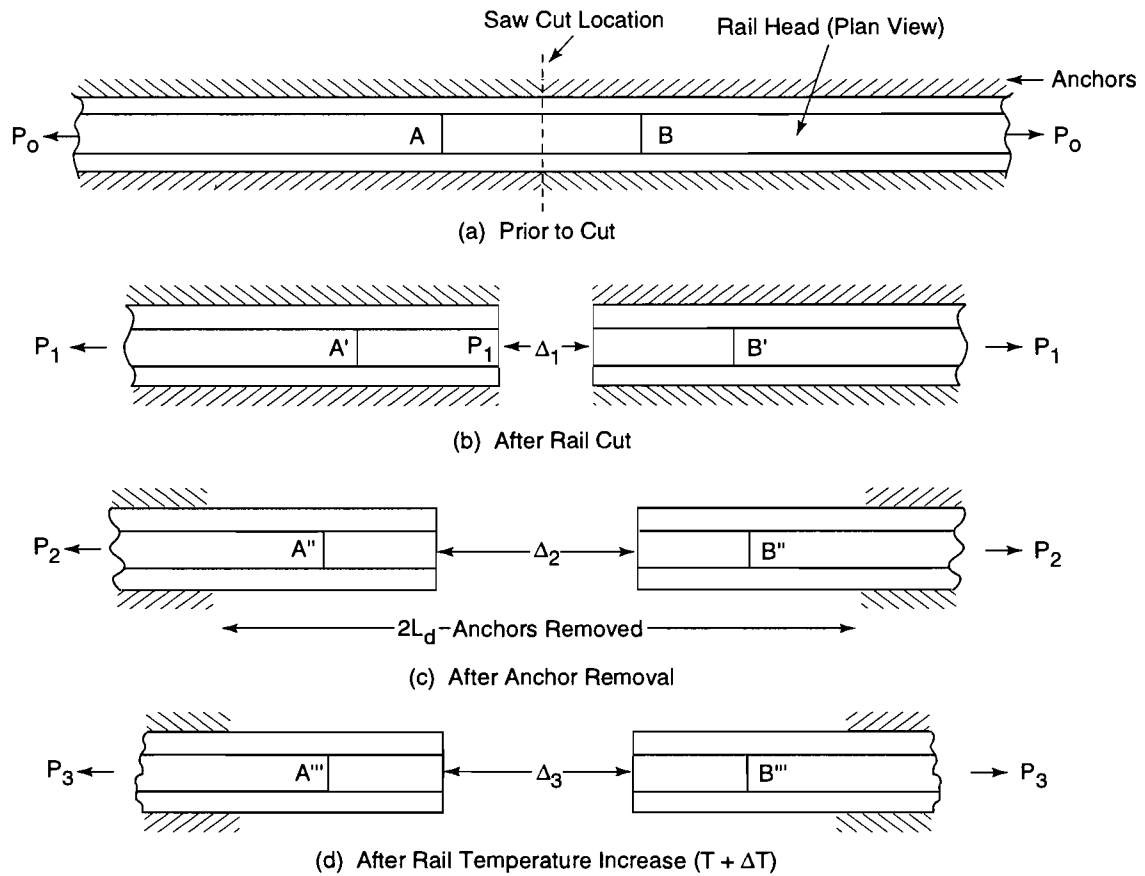
For the fifth test, one-half of the track had ETA on both rails, and the other half had EOTA. This setup was intended to facilitate a direct comparison of the longitudinal restraint behavior of the rails under the two important anchoring patterns, contributing to different longitudinal resistances.

The initial neutral temperature prior to cut was intentionally set at a high value to obtain large tensile load in the rail when the temperature was low in early mornings. All the testing, including the initial neutral temperature setup, was performed under the diurnal heating and cooling conditions of the rails. No artificial heating or hydraulic tensioning of rails was employed. The WRB tests were performed at about 6 a.m. on different days during the test period activity to obtain the lowest rail temperatures possible.

3.2 TEST CONDUCT

All the displacement transducers were zeroed prior to rail cuts. Two scribe marks about 2 ft apart were made on the rail head on either side of the central cut location, prior to saw cutting. The distance between the marks was measured soon after the cut and the difference from the initial value represented the gap, Δ , which was correlated with the displacement transducer data. The track operations and the gap definition are schematically illustrated in Figure 3-2. The rail force distribution, the displacements and temperature were recorded in each of the operations, viz., prior to rail cutting, soon after rail cut, after the removal of anchors over a specified length and finally, after some rail temperature increase due to solar heating.

Comparing the rail force distributions before and after the rail cuts, the required deanchoring length $2L_d$ was determined on the basis that the change in the rail force in the anchored section (beyond $2L_d$) was no more than 20 kips (see Figure 2-4b). The track was deanchored up to this length, except in cases where the limit was not reached in the test zone, for which the entire test length (1200 ft) was deanchored.



267-DTS-09718-4

Figure 3-2. Definition and Measurement of Rail Gap

3.3 WRB TEST DATA AND ANALYSIS

3.3.1 Test Data

The data recorded in each of the individual WRB tests are provided in the following subsections. For each test condition, the rail force and the displacements were collected at all instrumented locations for the three conditions of 1) prior to rail cut, 2) after rail cut, and 3) after deanchoring of the section.

A summary of the recorded test data, including rail force, gap size, deanchored length, and temperature, is provided in Table 3-2 by test number. The track section configuration, either EOTA or ETA, is also shown. The gap lengths listed (initial and after anchor removal) are the measured gaps between the cut rail ends. The displacements of the rail ends used for the analytical model are based on closest transducer data, extrapolated to the cut location. In some

Table 3-2. Test Data

Test No.	Anchor Pattern		Gap (in.)	u_0 (in.)		P_0 (kips)	λ (lb/in.)	
	Test Rail	Other Rail		Left	Right		Left	Right
WRB1	EOTA	EOTA	3.26	1.61	1.65	193	9.25	11.50
WRB2	EOTA	EOTA	3.45	1.70	1.75	190	11.00	9.50
WRB3	EOTA	EOTA	1.81	0.90	0.91	115	2.00	0.50
WRB4	EOTA	ETA	1.81	0.81	1.00	141	12.75	5.50
WRB5a	ETA	ETA	2.37	0.95	NA	166	6.00	NA
WRB5b	EOTA	EOTA	2.37	NA	1.42	166	NA	6.00

tests, the displacements were measured at the cut location directly using a transit. Table 3-2 presents the values of λ (negative slope of the linearized initial force distribution, as shown in the Appendix).

Figures 3-3 and 3-4 show the rail force data for WRB tests 1 and 2 prior to rail cutting, soon after the cut and after anchor removal. Similar data were collected for all the tests. The data show that the initial rail force was not uniform and reduces over some distance from the center. This is attributed to inadequate destressing of CWR. For theoretical analysis the initial rail force distribution was fitted by a linear equation as described in Section 2. The overall fit is considered to be reasonable for the type of analysis presented here.

Clearly, the rail cut influenced the rail force distribution over a long distance in the test section. Removal of anchors over the test section further reduced the locked up stresses, though the effect of friction between rail and tie plates was noticeable in Figures 3-3 and 3-4. There was some increase in the rail temperature ($\approx 6^\circ\text{F}$) during anchor removal.

3.3.2 Analysis

Deanchored Section Lengths, L_d

Table 3-3 gives a summary of analysis predictions based on expressions (2-9.3) and (2-9.4). This table gives predicted L_d and f_0 for left and right halves of the test rail. The resulting change in force ΔP as measured in the tests, at these theoretical L_d values, is also shown in this table. Except for the first test, the ΔP force values ($P_i - P_f$) are small (below 20 kips); therefore, for all practical purposes, the initial force in the rail P_i is unaffected beyond the theoretical value of L_d . Hence, deanchoring up to L_d is required; this value should be considered as the minimum required deanchored section length. The longitudinal displacement at and beyond L_d is also found to be negligible as illustrated in the test versus theory correlations presented in Figures 3-5 to 3-16.

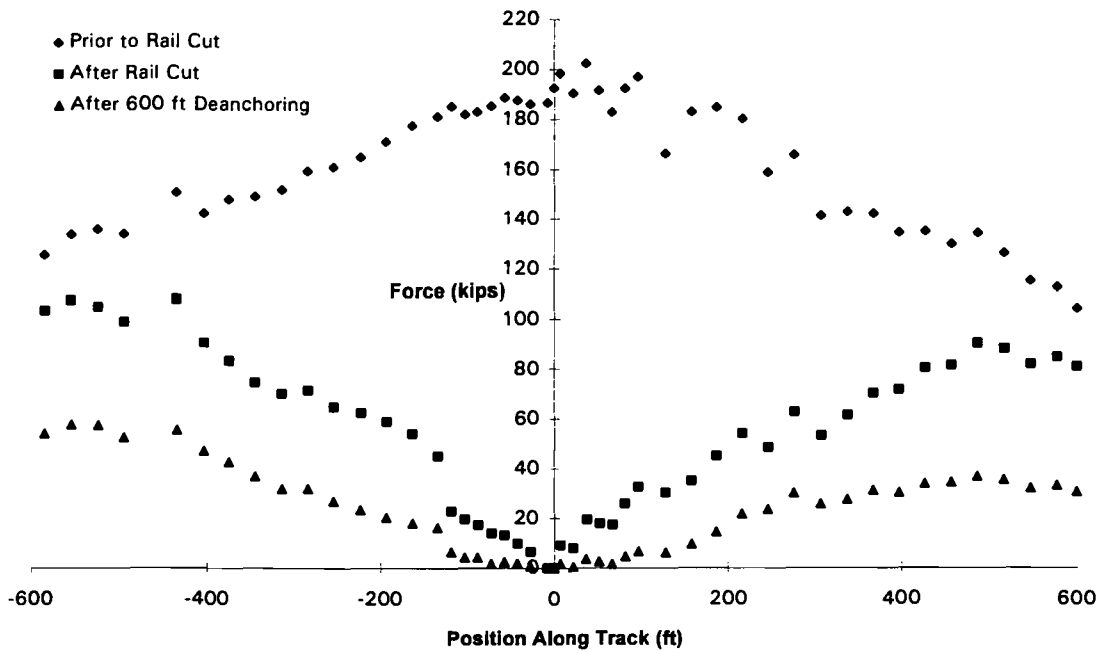


Figure 3-3. WRB1 Rail Force Data

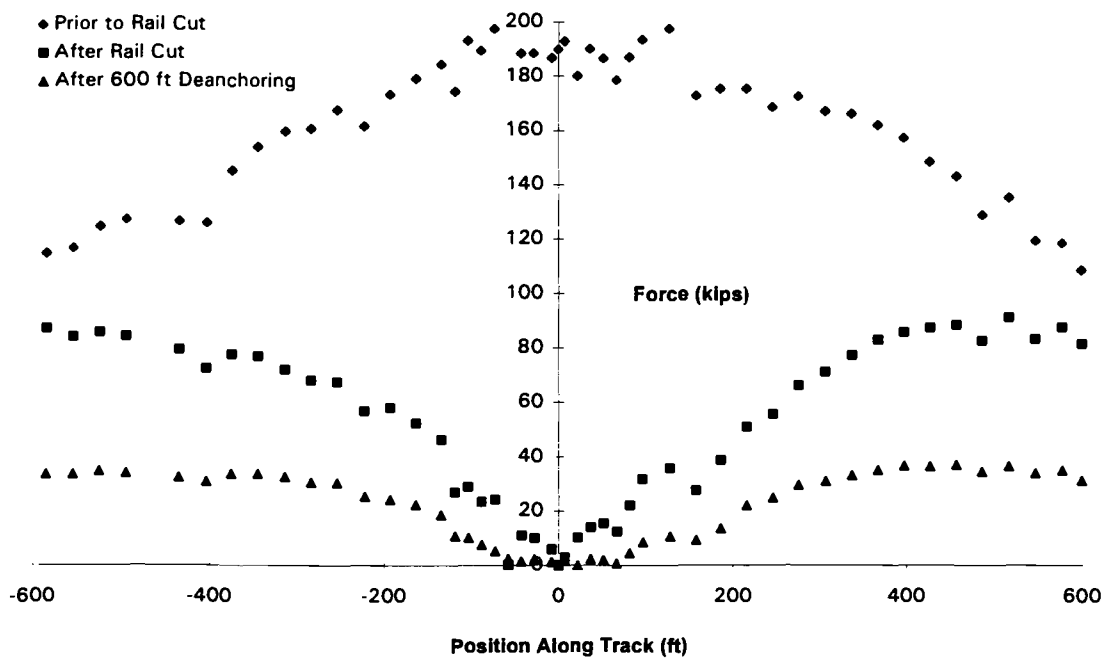


Figure 3-4. WRB2 Rail Force Data

Table 3-3. Analysis Predictions

Test No.	Anchor Pattern		f_0 (lb/in.)		L_d (ft)		Test ΔP at L_d	
	Test Rail	Other Rail	Left	Right	Left	Right	Left	Right
WRB1	EOTA	EOTA	20	17	557	571	49*	27
WRB2	EOTA	EOTA	16	16	597	615	19	17
WRB3	EOTA	EOTA	16	18	522	528	10	12
WRB4	EOTA	ETA	18	19	382	472	20	15
WRB5a	ETA	ETA	30	NA	381	NA	19	NA
WRB5b	EOTA	EOTA	NA	18	NA	569	NA	18

*Test data suspect.

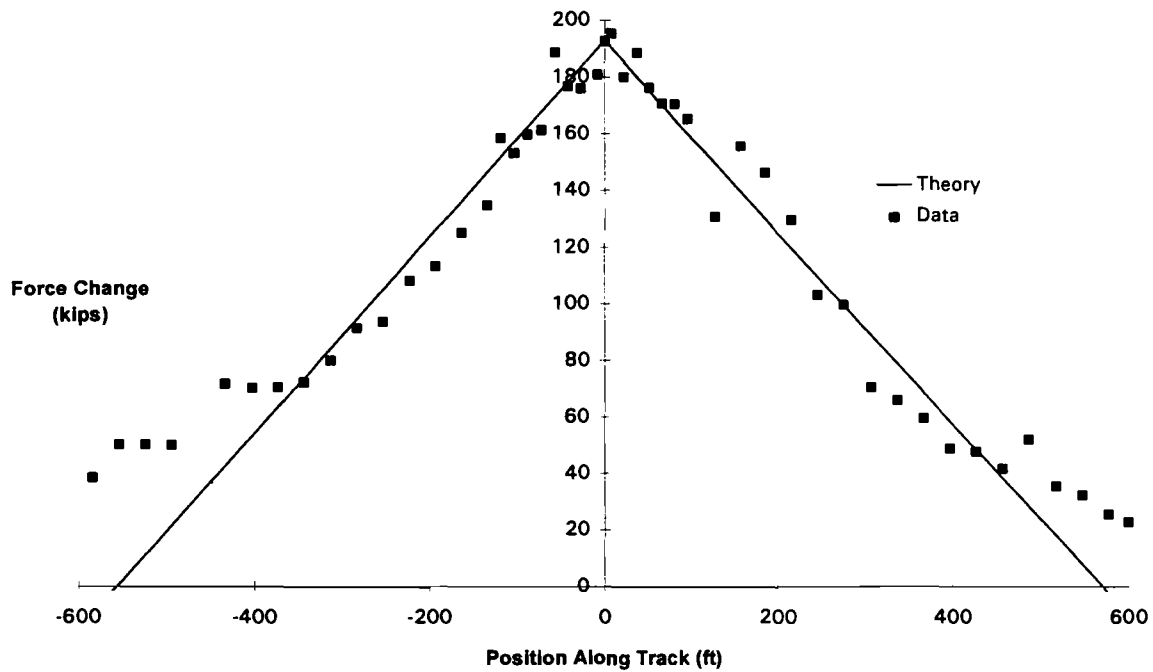


Figure 3-5. WRB1 Rail Force Change Due to Cut

The first test showed some discrepancy from the theoretical L_d . Figure 3-5 shows that the test force data did not exhibit a monotonic behavior at the test zone ends (> 400 ft). This is attributed to instrumentation and other possible sources of error in the test setup.

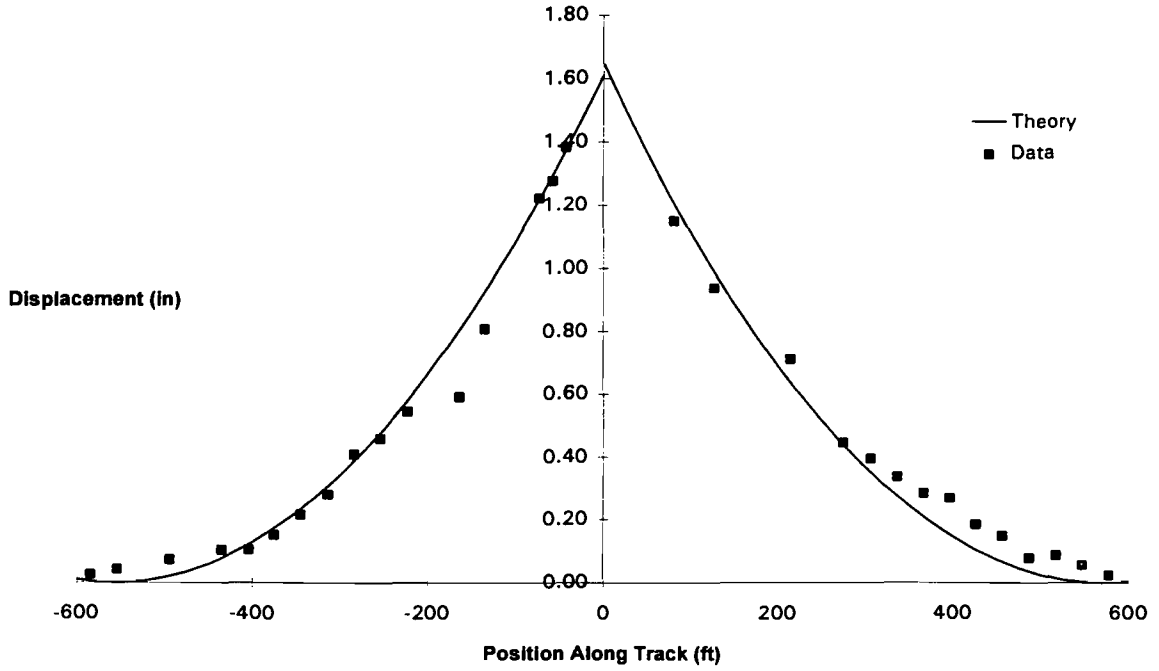


Figure 3-6. WRB1 Rail Displacement Due to Cut

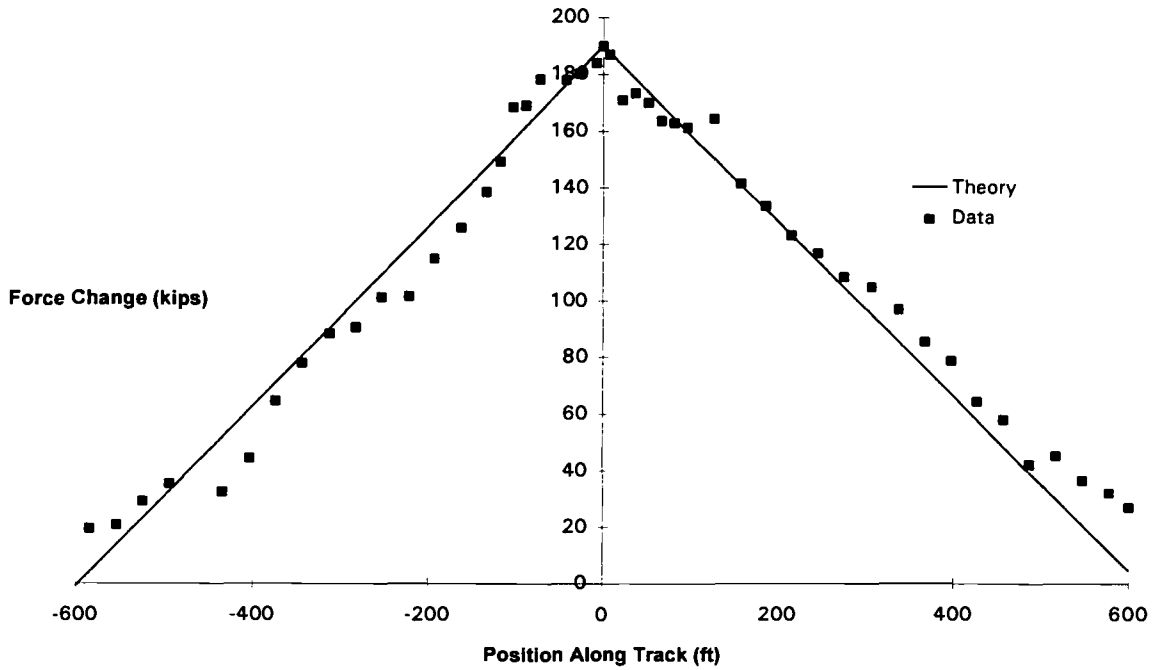


Figure 3-7. WRB2 Rail Force Change Due to Cut

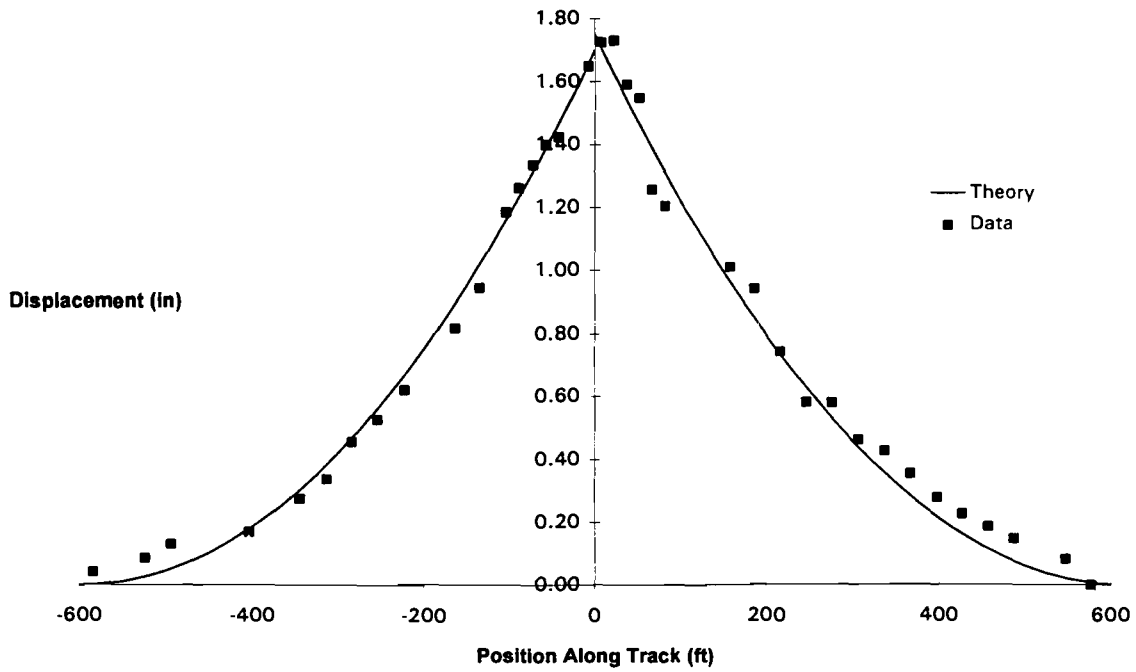


Figure 3-8. WRB2 Rail Displacement Due to Cut

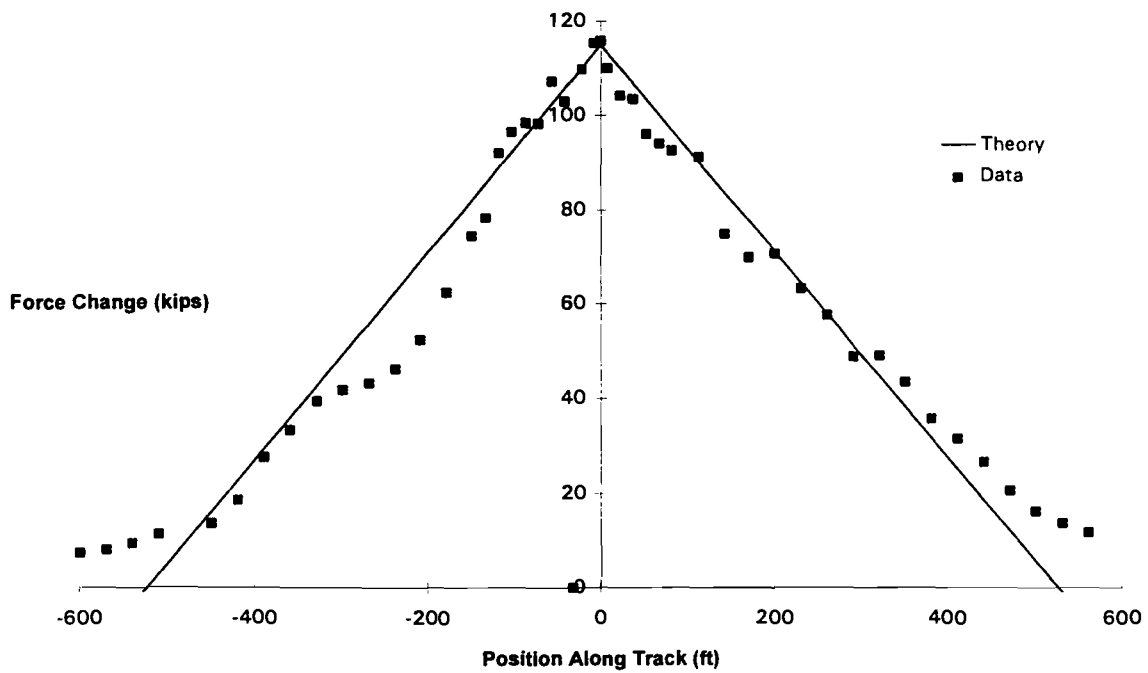


Figure 3-9. WRB3 Rail Force Change Due to Cut

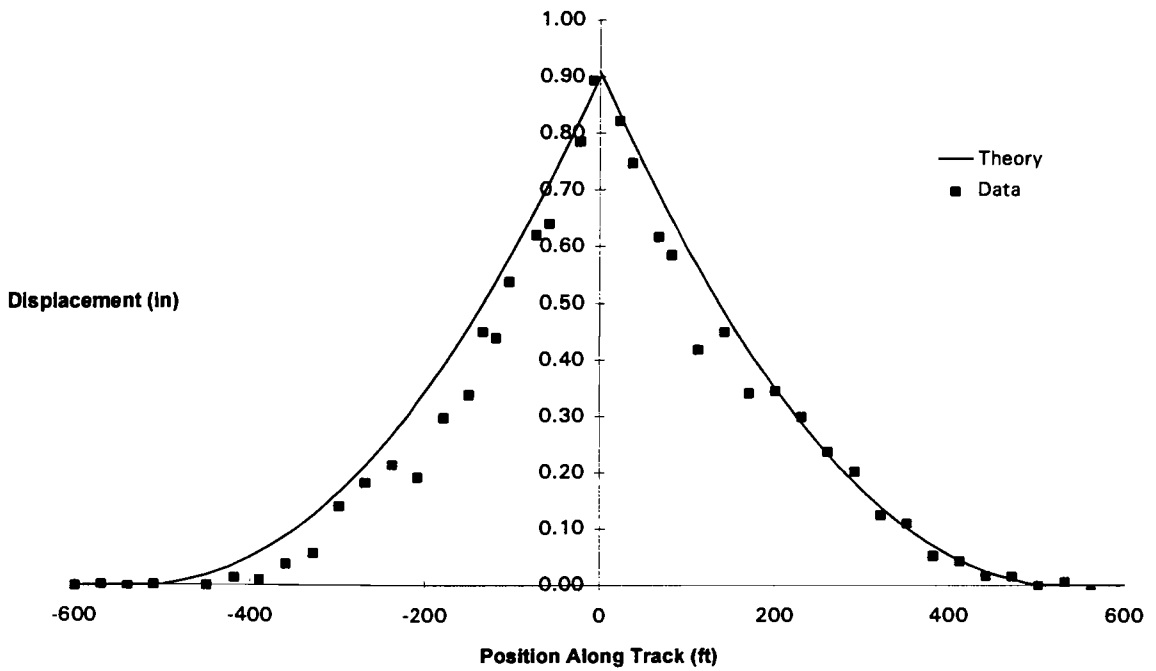


Figure 3-10. WRB3 Rail Displacement Due to Cut

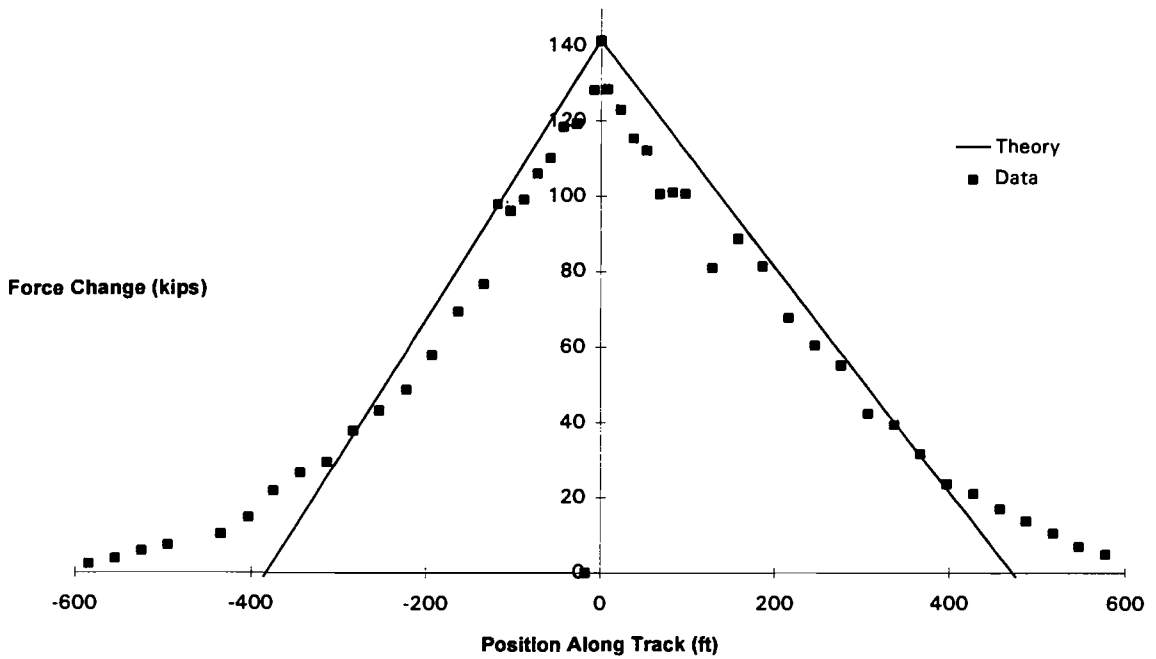


Figure 3-11. WRB4 Rail Force Change Due to Cut

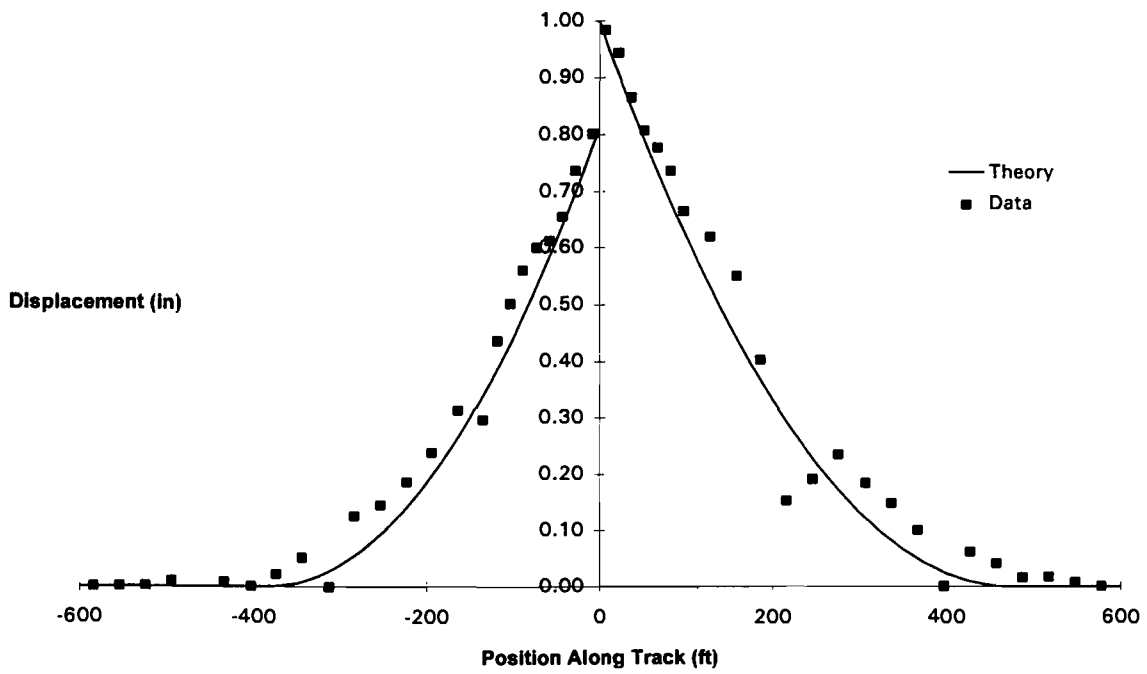


Figure 3-12. WRB4 Rail Displacement Due to Cut

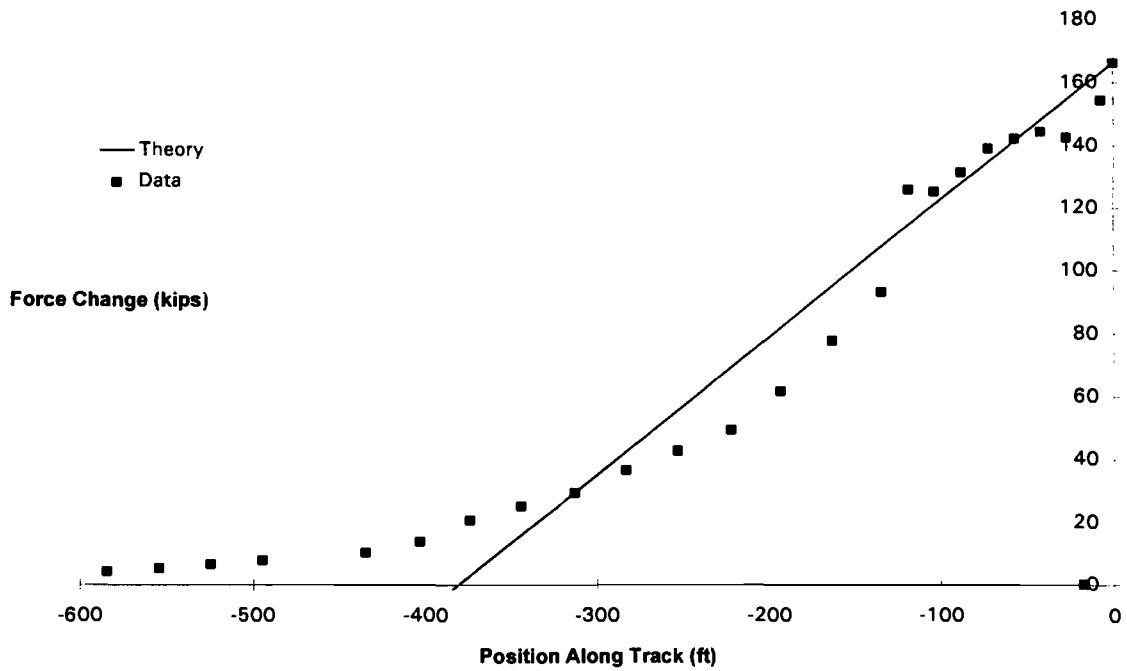


Figure 3-13. WRB5a Rail Force Change Due to Cut (ETA)

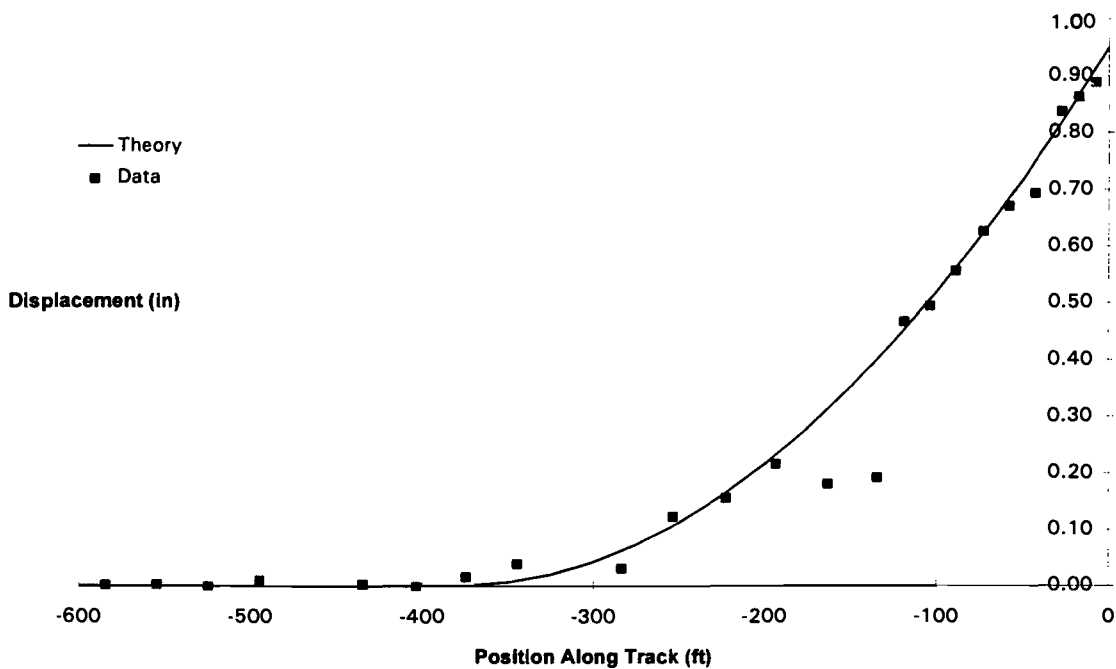


Figure 3-14. WRB5a Rail Displacement Due to Cut (ETA)

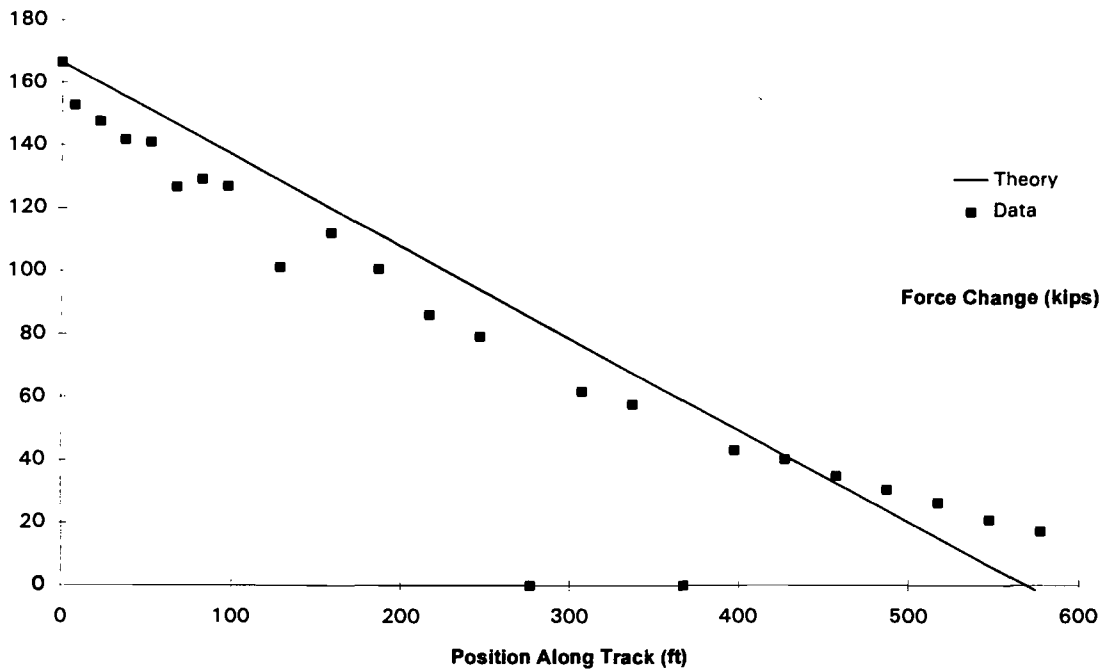


Figure 3-15. WRB5b Rail Force Change Due to Cut (EOTA)

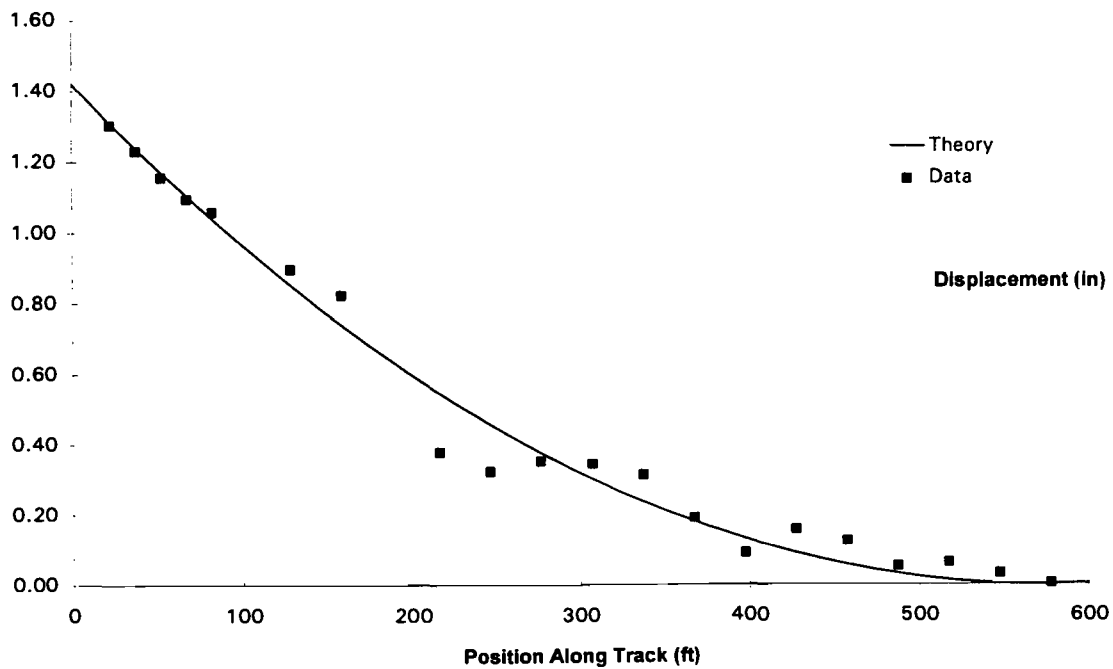


Figure 3-16. WRB5b Rail Displacement Due to Cut (EOTA)

Longitudinal Resistance, f_0

The resistance values calculated and presented in Table 3-3 show that the range of resistance for the EOTA pattern is 16 to 20 lb/in. Ignoring the result from WRB4, which has different anchoring patterns on the test and the other rail, the average resistance for EOTA (on the basis of WRB1, WRB2, WRB3, and WRB5b) is found to be about 17 lb/in. For the anchor pattern with ETA there is only one test result (WRB5a) which is 30 lb/in., which is about twice EOTA, as one would expect. In tests 5a and 5b, the deanchored section length for ETA is not half of the EOTA section (381 ft versus 569 ft) but has the ratio of about 2/3. This is attributed to finite λ , which represents the rate at which the initial force drops off with distance from the cut location. The theoretical Equations (2-9.3) and (2-9.4) show that the deanchored section length would vary inversely with the sum of λ and f_0 . For test 5a and 5b ($f_0 = 30$ lb/in., 18 lb/in., $\lambda = 6$ lb/in.), the deanchored section lengths ratio works out to be 2/3.

Correlation with Force and Displacement Fields

Detailed test and theoretical correlations on force change and displacement fields are presented in Figures 3-5 to 3-16. The test data in some cases do not exhibit smooth monotonic behavior either due to instrumentation errors or due to local irregularities in track conditions. The theoretical force change distribution is linear which reasonably correlates with the test data at least up to a distance of L_d . The test displacement field is reasonably well represented by the theoretical parabolic distribution, in many cases. Hence it is concluded that the proposed theory, which is computationally simple, is adequate for application in the practical situations.

It is also noted that the deanchored rail sections experience some tie plate friction. As seen in Figures 3-2 and 3-3, there is a force built up of about of 20 kips over a length of 400 ft, representing about 4 lb/in. frictional resistance. This can be reduced by rail vibration or mounting rails on rollers, which is the European railroad practice not currently used in the U.S. industry.

3.3.3 Key Findings

1. Analytical predictions of the longitudinal response under the Winter Rail Break conditions are in reasonable agreement with the test data. The resistance idealization as a constant seems to be adequate.
2. The longitudinal resistance to the rail movement depends on the anchoring pattern. ETA gives about twice the resistance of EOTA. The resistance to the cut rail is apparently influenced by the anchoring pattern of the other rail. If the other rail is also cut it can reduce the resistance offered to the rail under investigation. These influences were observed in the tests but not quantified in the present report.
3. The required deanchored section length is considered to be the rail force disturbance zone due to the cut. Beyond this length the rail force is not significantly affected. The deanchored section length increases with increasing initial rail force at the cut location and reduces with the increased longitudinal resistance from the anchors and the ballast. This length is also influenced by the initial rail force distribution (i.e., λ , the negative slope of the linearized distribution). Within the assumption that the resistance is constant and the initial force distribution linear, one can calculate the required deanchored length on the basis of the initial rail force level at the cut location and the longitudinal displacements at this location. It is not necessary to know the complete initial force distribution in this calculation.
4. The deanchored lengths and the rail gap size observed in the test are underestimates for the cases when the initial force distributions are constant. To illustrate this, consider the WRB2 test as an example. The average longitudinal resistance (left and right side of the cut) is about 16 lb/in. The initial force at the cut location is 190 kips in this test. Had this force been constant, the required deanchored length would have been 990 ft on either side of the cut. In the test the deanchored length was about 600 ft. This reduction is due to the drooping initial force that existed in the test rail. Likewise, the rail gap measured in the test (≈ 3.5 in.) is lower compared to the expected value of 5.6 in. ($P_0^2/2f_0AE$), had the initial force remained uniform throughout the test section. Hence, rail gaps on this order are possible due to winter rail fracture in some situations.

4. SUMMER RAIL DESTRESSING INVESTIGATIONS

The test conduct and test measurements are briefly described here, followed by a test data summary and analytic correlations.

4.1 TEST SETUP

The tests were conducted on the same section used for the WRB tests. In fact, the testing alternated between the WRB and SRD scenarios, with appropriate rail neutral temperatures to obtain the desired tensile or compressive loads at the rail cutting temperatures. The instrumentation setup was the same as described in Section 3 for the WRB tests.

The test matrix shown in Table 4-1 consists of seven tests. The first two and the last two tests simulated the EOTA pattern on the test rail and on the other rail. The third test simulated the ETA pattern on the test rail and an EOTA pattern on the other rail. The fourth test simulated the ETA pattern on the test rail and no anchoring on the other rail. The first five tests had the same used anchors. In the sixth and seventh tests, new reformed anchors were employed.

For the fifth test, one-half of the track had ETA on both rails, and the other half had EOTA. This setup was intended to facilitate a direct comparison of the longitudinal restraint behavior of the rails under the two important anchoring patterns.

The initial neutral temperature was intentionally set low to obtain large enough compressive loads in the rail when the rail temperature was high. The SRD tests were performed typically between 2 to 3 p.m. when the rail temperature reached its maximum.

Table 4-1. Summer Rail Destressing Test Matrix

Test No.	Anchor Pattern		Approximate T_N at Center (°F)	Approximate Rail Cut Temperature, T_C (°F)	Comment
	Test Rail	Other Rail			
SRD1	EOTA	EOTA	70	130	{ Tests at moderate force levels
SRD2	EOTA	EOTA	70	130	
SRD3	ETA	EOTA	70	130	
SRD4	ETA	None	70	130	
SRD5a	ETA	ETA	<50	>100	{ Provide direct comparison of EOTA versus ETA
SRD5b	EOTA	EOTA	<50	>100	
SRD6	EOTA	EOTA	65	108	{ Re-formed anchors used
SRD7	EOTA	EOTA	65	108	

4.2 TEST CONDUCT

The rail was first torch cut, followed by finishing saw cuts at the two faces. The cutout length of steel varied from test to test (from about 2 to 3.5 in.). The rail longitudinal displacement, and the resulting gap were measured and correlated with the cutout length. Figure 4-1 represents the gap and displacements in the track operations (rail cutting, steel removal and deanchoring).

The deanchored length $2L_d$ was based on the criterion that the change in the rail force in the deanchored zone was less than 20 kips prior to deanchoring.

The rail temperature, force distribution, the rail longitudinal displacements and the gap were all recorded during the operations of the test. The force distribution during the operations is similar to that shown in Figure 2-4.

4.3 SRD TEST DATA AND ANALYSIS

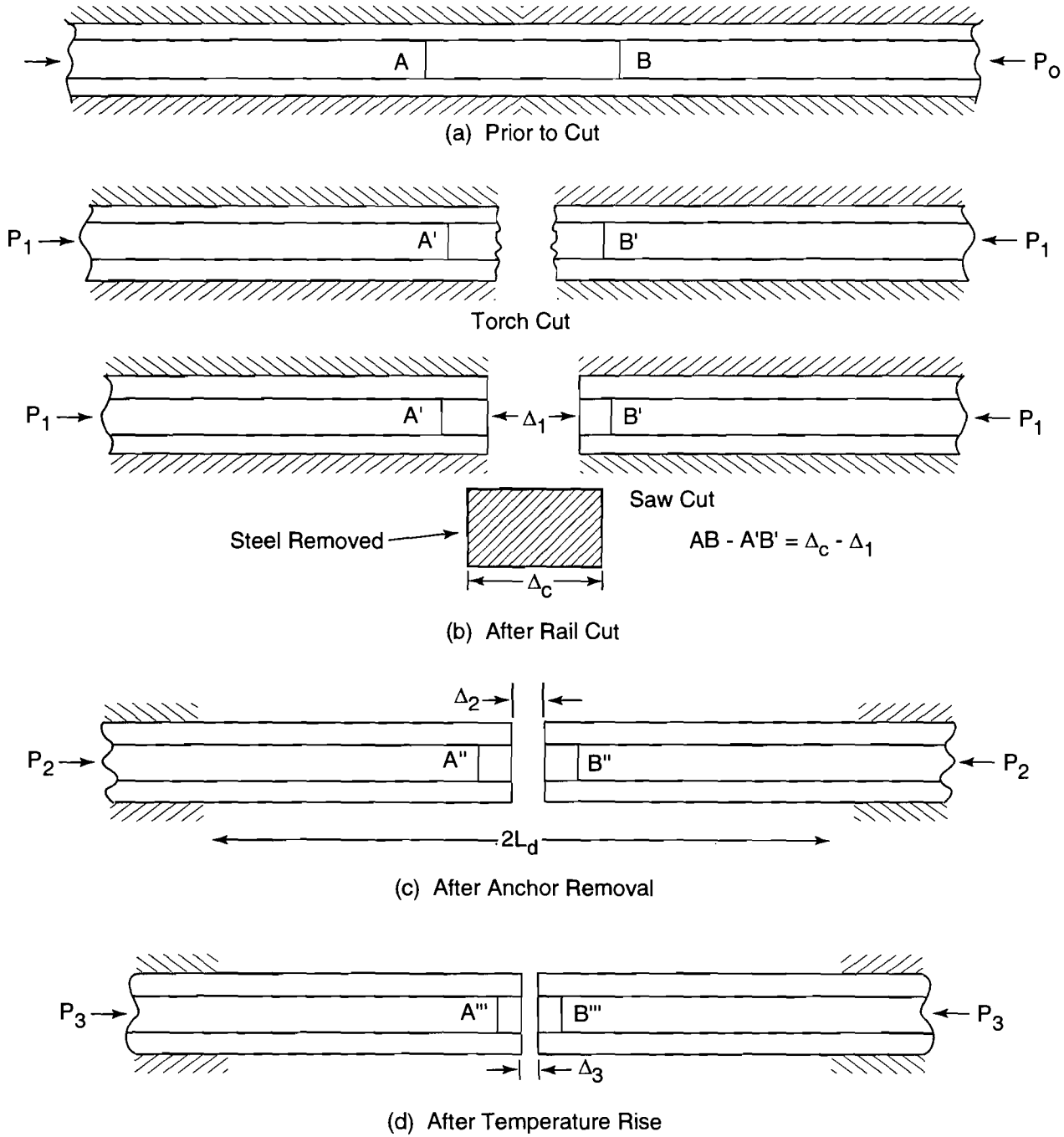
4.3.1 Test Data

The data recorded in each of the SRD tests are provided in the following subsections. As with the WRB tests, the force and displacement data at all instrumented locations were collected for the three conditions: 1) prior to rail cut, 2) after rail cut, and 3) after deanchoring of the section. Utilizing the rail force and displacement data after cut, the track model was exercised to calculate the longitudinal resistance and the target deanchoring length.

A summary of the recorded test data, including rail force, gap size, deanchored length, and temperature, is provided in Table 4-2 by test number. The track section configuration, either EOTA or ETA, is also shown. The gap lengths listed (initial and after anchor removal) are the measured gaps between the cut rail ends. Unlike the WRB tests where the saw cut rail contracts to leave a larger gap, the SRD tests require torch cutting of the rail followed by additional cutting to remove a plug section from the rail to allow for free expansion. The gap and the length of steel removed are shown in the table. The rail displacement at the cut locations for the analytical model is based on extrapolation of the rail deflection data from the adjacent displacement transducers.

As in the WRB analysis, the rail force data for tests prior to rail cutting, soon after the cut and after anchor removal were examined. The data show that the initial rail force was not uniform. This is attributed to inadequate destressing of CWR. For theoretical analysis the initial rail force distribution was fitted by a linear equation as described in the Appendix. The overall fit is considered to be reasonable.

The rail cut influenced the rail force distribution up to L_d . Removal of anchors over the test section further reduced the locked up stresses.



267-DTS-09718-3

Figure 4-1. Definition and Measurement of Cutout Length and Rail Gap

Table 4-2. Test Data

Test No.	Anchor Pattern		Removed Steel (in.)	Gap (in.)	u_0 (in.)		P_0 (kips)	λ (lb/in.)	
	Test Rail	Other Rail			Left	Right		Left	Right
SRD1	EOTA	EOTA	3.45	2.26	0.64	0.55	128	8.75	17.50
SRD2	EOTA	EOTA	2.43	1.20	0.65	0.58	111	8.25	15.25
SRD3	ETA	EOTA	2.22	1.44	0.36	0.42	89	9.50	10.00
SRD4	ETA	None	2.69	1.13	0.75	0.81	125	9.50	10.00
SRD5a	ETA	ETA	1.94	0.45	0.78	NA	124	-5.00	NA
SRD5b	EOTA	EOTA	1.94	0.45	NA	0.71	124	NA	13.00
SRD6	EOTA	EOTA	6.07	4.02	0.95	1.10	134	0.25	1.00
SRD7	EOTA	EOTA	5.42	4.02	0.65	0.75	126	0.04	6.25

4.3.2 Analysis

Deanchored Section Lengths, L_d

Table 4-3 gives a summary of analysis predictions based on expressions derived in Section 2. This table gives predicted L_d and f_0 for left and right halves of the test rail. The resulting change in force ΔP as measured in the tests, at these theoretical L_d values, is also shown in this table. This is found to be small and below the 20 kip limit. Therefore for all practical purposes, the initial rail force is not affected by the rail cut beyond the theoretical L_d . The longitudinal displacement beyond L_d is also found to be negligible as shown in Figures 4-2 to 4-17 for all the Summer Destressing tests.

Longitudinal Resistance, f_0

The average longitudinal resistance for the EOTA pattern on both rails (average of SRD1, SRD2 and SRD5b) works out to be about 17 lb/in. (test results from SRD6 and SRD7 are not included in this average because in these tests newly re-formed anchors were employed and additional care was exercised to squeeze tight the anchors). This average is the same as obtained in WRB tests for EOTA conditions. If test data from SRD6 and SRD7 are also included, the average will be 19 lb/in.

For the anchor pattern with ETA the test SRD3 gave a result which is unduly low, possibly due to EOTA condition on the other rail. Likewise, SRD4 gave a low value since the other rail was not anchored, which resulted in slight in-plane rotation of the ties. Thus, when the anchoring pattern of the other rail is not similar to the test rail, some discrepancy in the calculated resistance value is apparent. The only relevant ETA condition is considered to be in the SRD5a test, which gave a value of 30 lb/in., which agrees with the result obtained from the WRB5a test.

Table 4-3. Analysis Predictions

Test No.	Anchor Pattern		f_o (lb/in.)		L_d (ft)		Test ΔP at L_d	
	Test Rail	Other Rail	Left	Right	Left	Right	Left	Right
SRD1	EOTA	EOTA	23	20	334	287	1	16
SRD2	EOTA	EOTA	15	11	391	349	-2	4
SRD3	ETA	EOTA	18	14	270	315	8	3
SRD4	ETA	None	17	14	401	433	-6	-1
SRD5a	ETA	ETA	30	NA	420	NA	-2	NA
SRD5b	EOTA	EOTA	NA	14	NA	382	NA	9
SRD6	EOTA	EOTA	23	19	474	548	0	7
SRD7	EOTA	EOTA	30	20	344	397	5	11

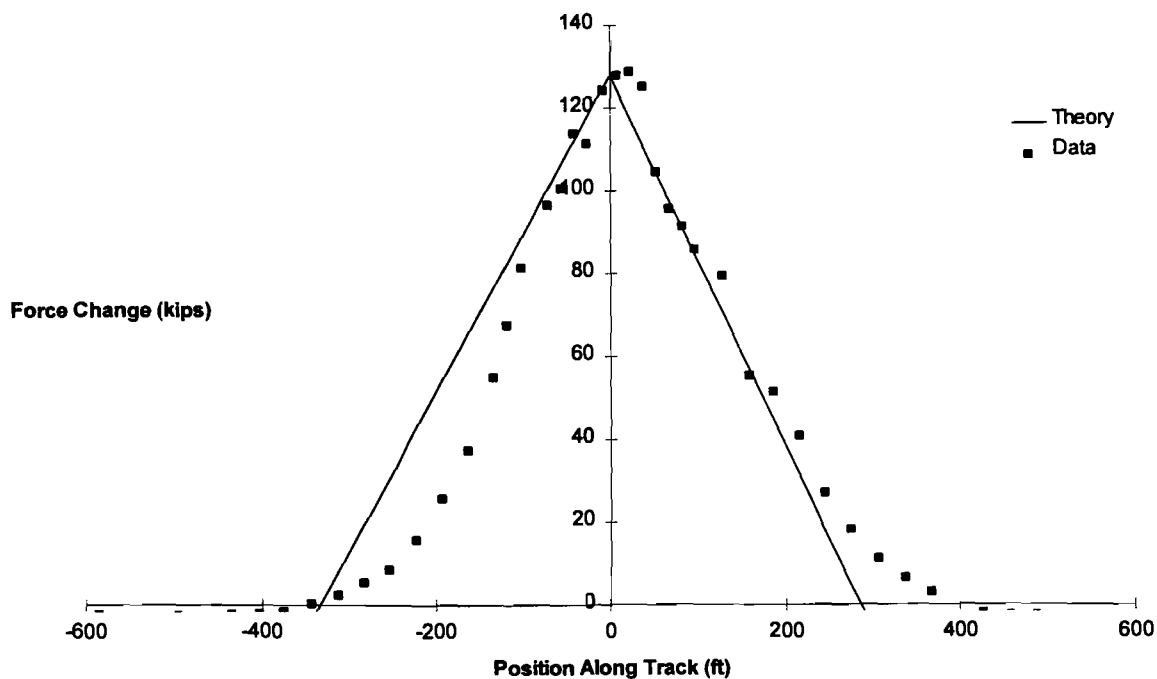


Figure 4-2. SRD1 Rail Force Change Due to Cut

The theoretical deanchored section length for EOTA and ETA on the basis of test 5a and 5b works out to be 0.9 and not 0.5. This is attributed to significant force distribution ($\lambda = -5$ and 13, respectively). As stated earlier in the discussion on Winter Rail Break conditions, the ideal ratio of 0.5 is realized only when $\lambda = 0$ (for uniform initial force distribution).

It is interesting to compare the results of SRD1 and SRD6. Both had the same anchoring pattern and nearly equal initial rail forces at the cut locations. The deanchored section lengths differ significantly due to λ differences in the force distributions.

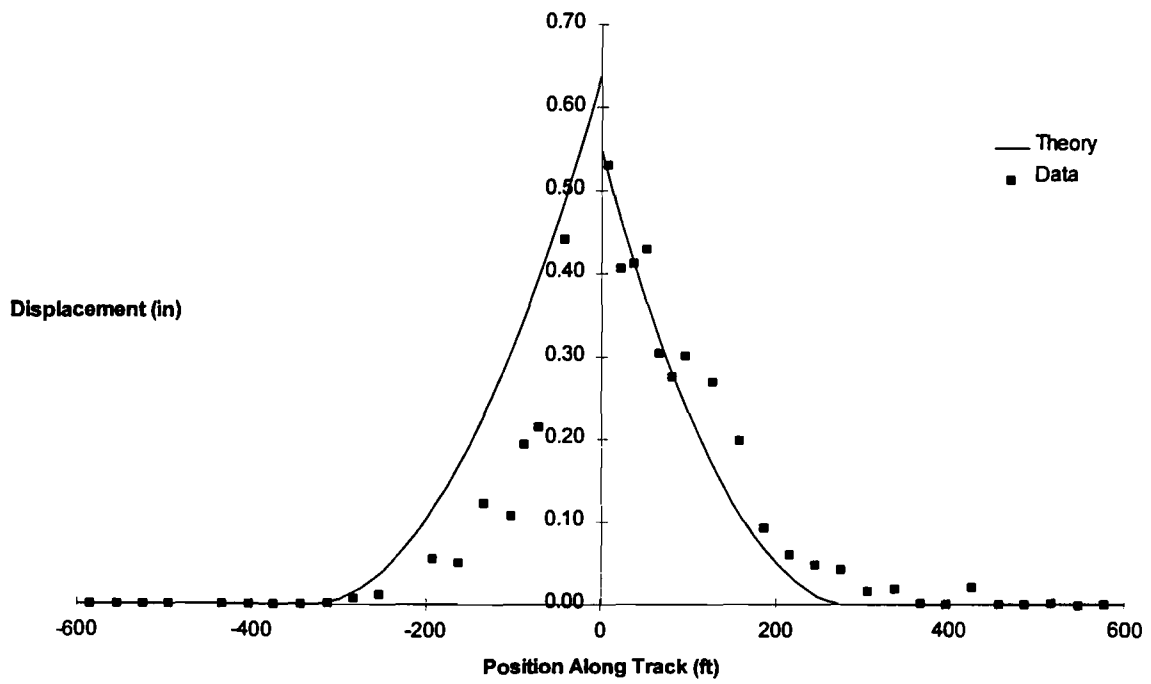


Figure 4-3. SRD1 Rail Displacement Due to Cut

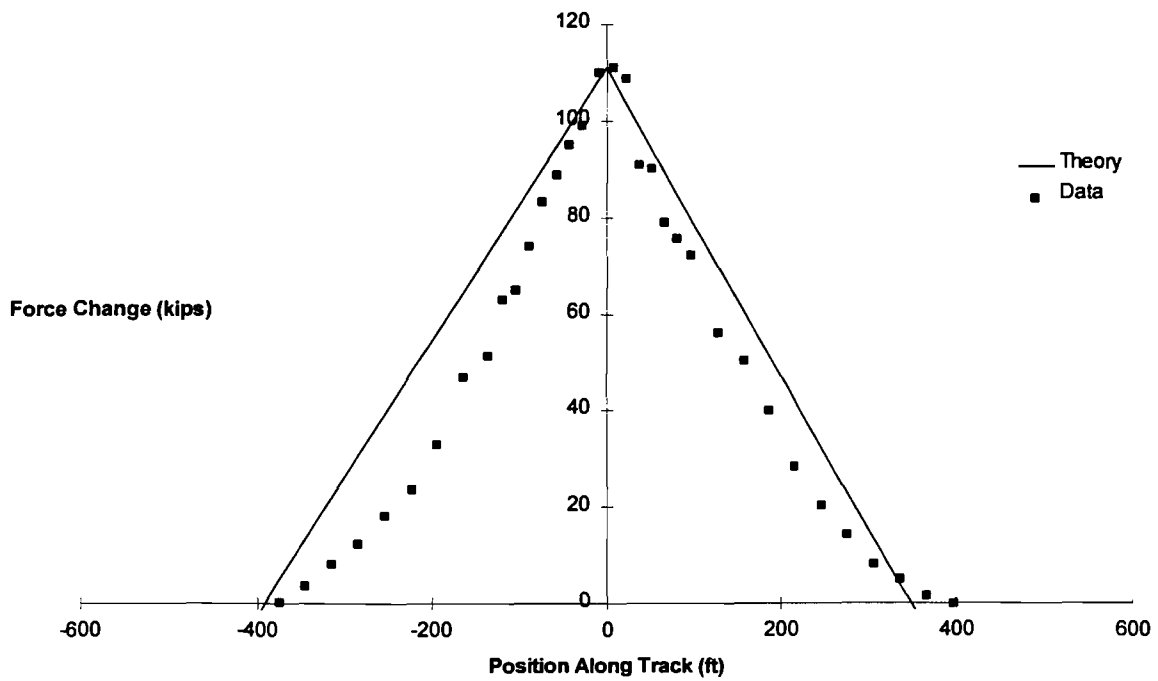


Figure 4-4. SRD2 Rail Force Change Due to Cut

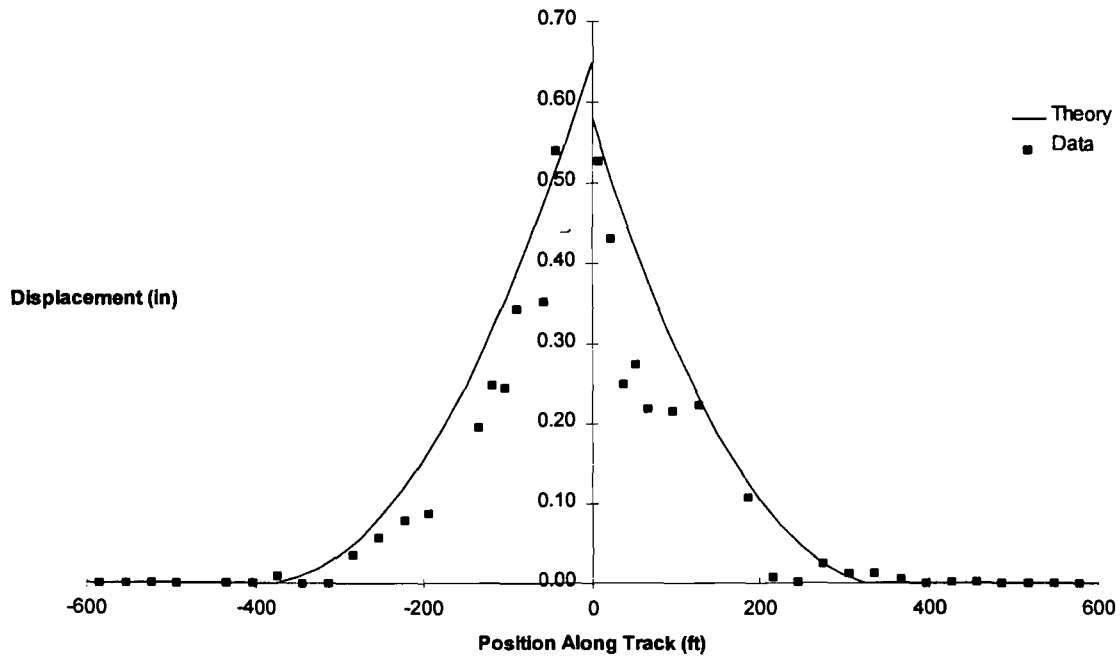


Figure 4-5. SRD2 Rail Displacement Due to Cut

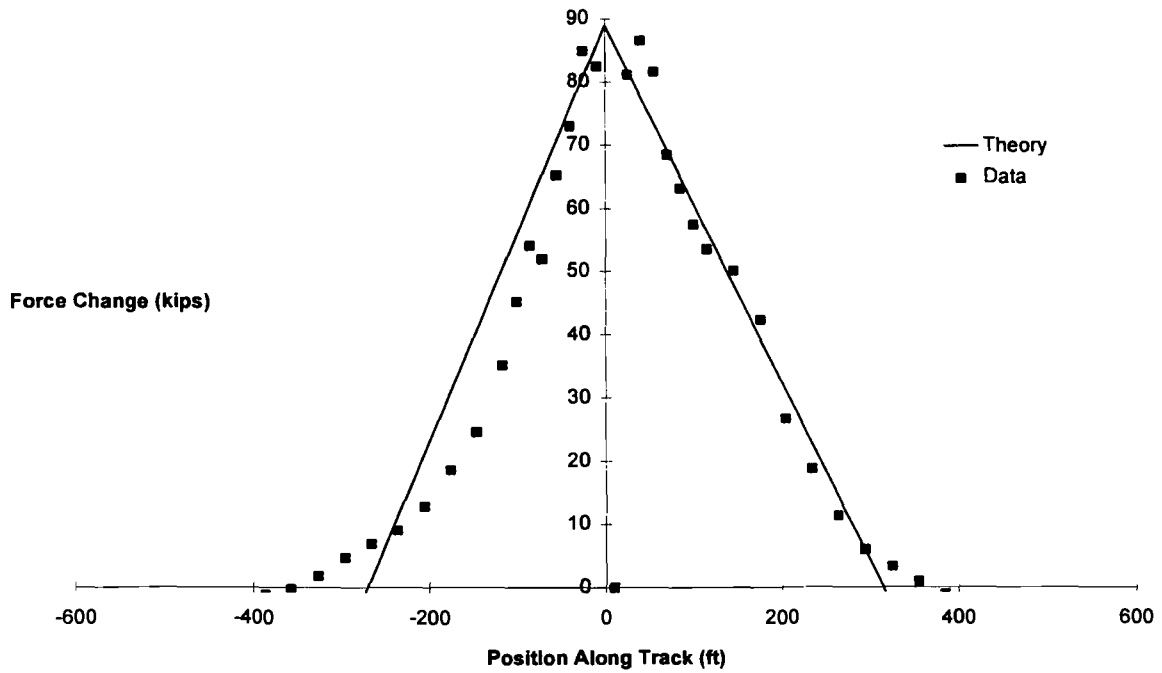


Figure 4-6. SRD3 Rail Force Change Due to Cut

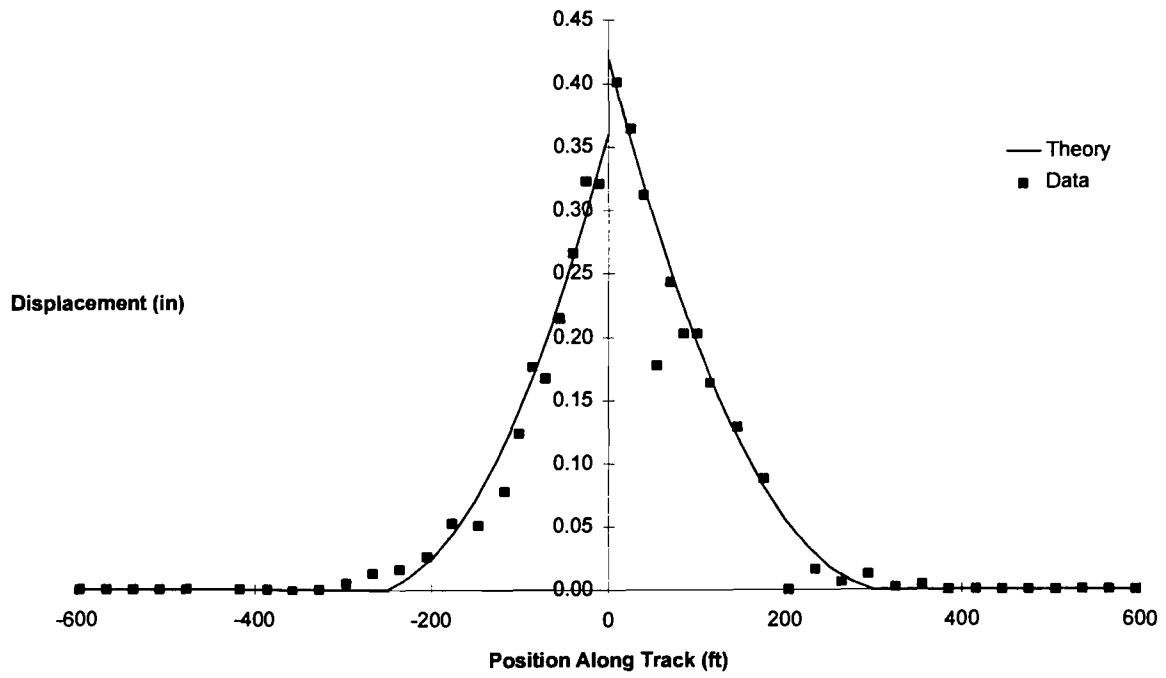


Figure 4-7. SRD3 Rail Displacement Due to Cut

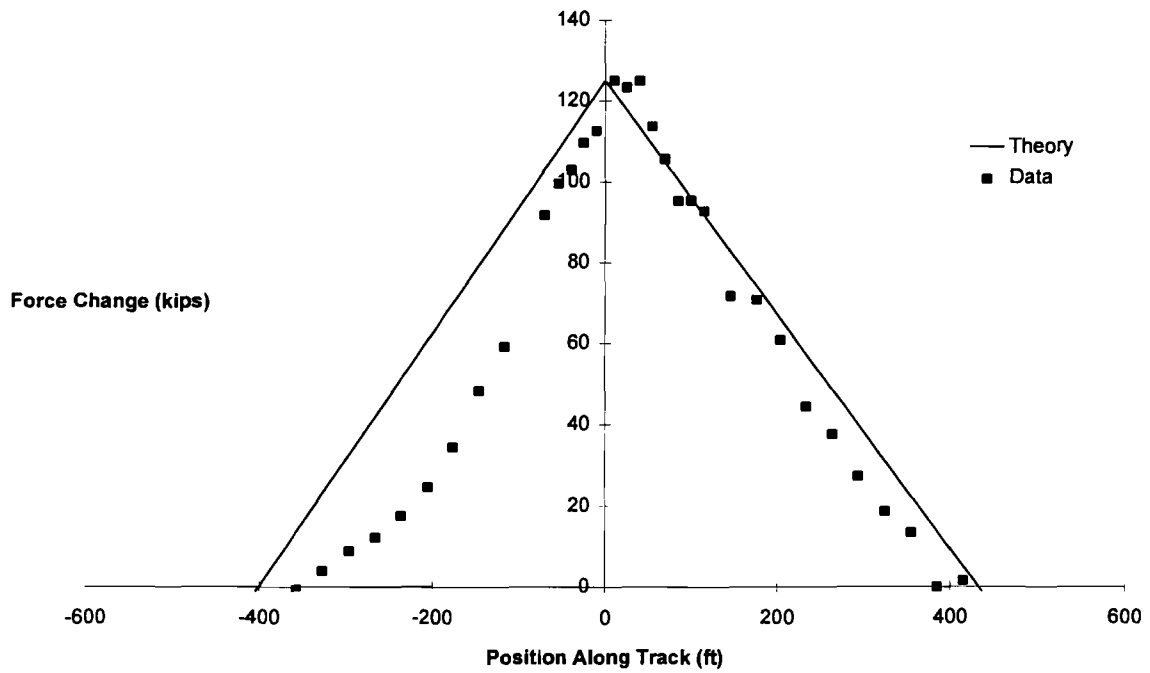


Figure 4-8. SRD4 Rail Force Change Due to Cut

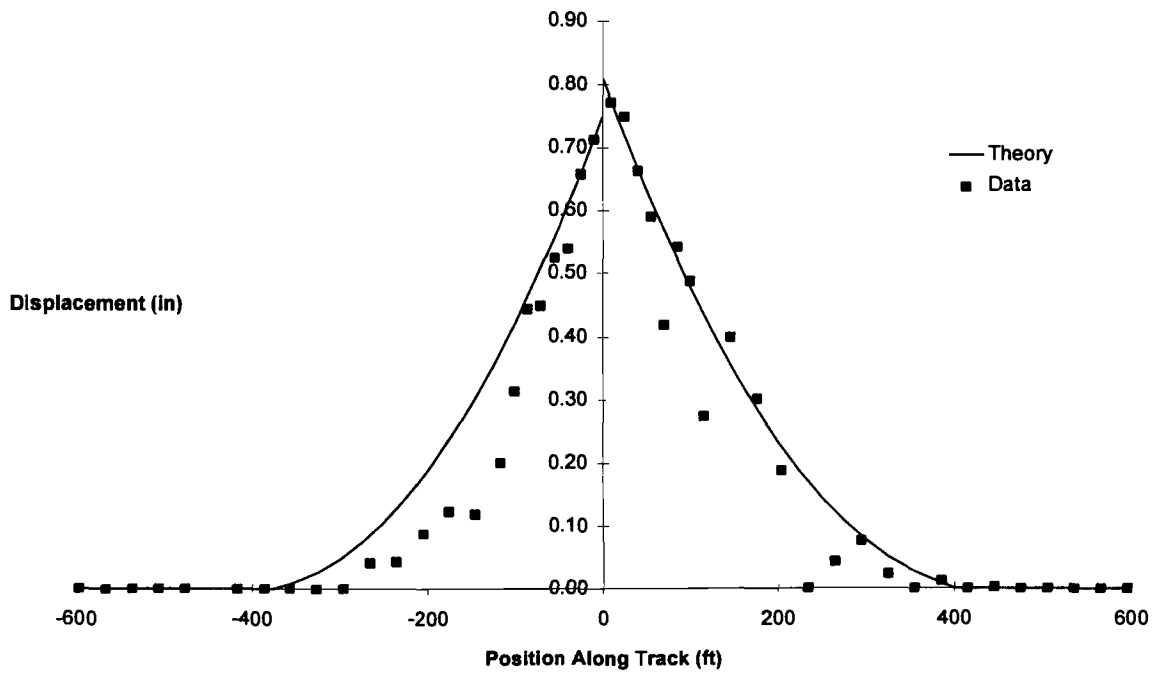


Figure 4-9. SRD4 Rail Displacement Due to Cut

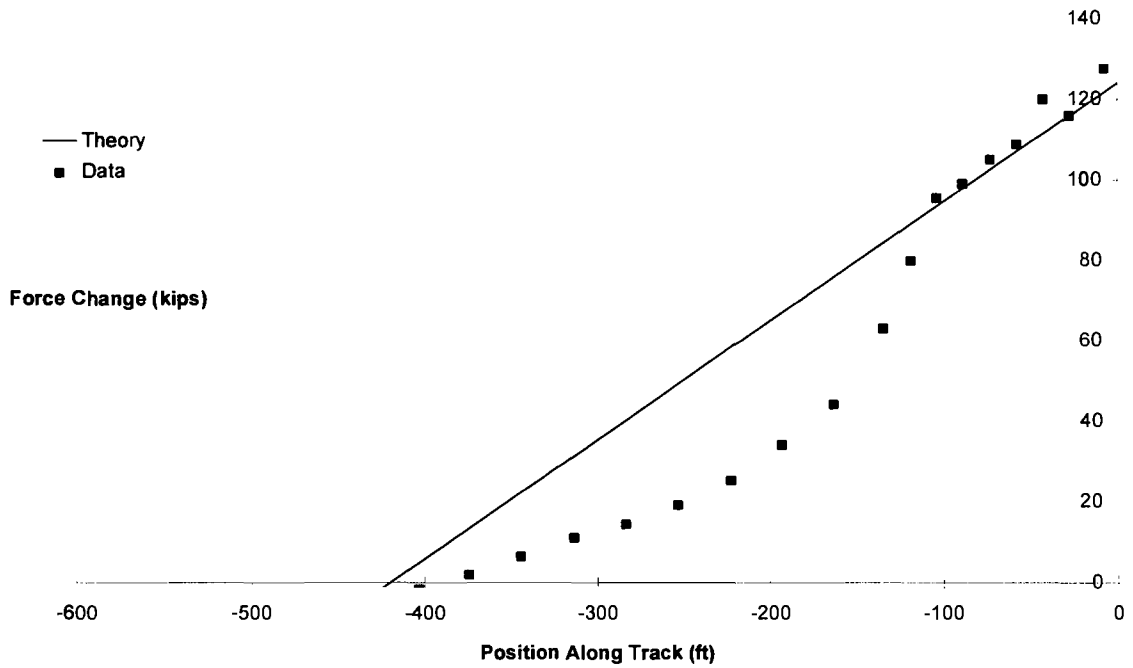


Figure 4-10. SRD5a Rail Force Change Due to Cut

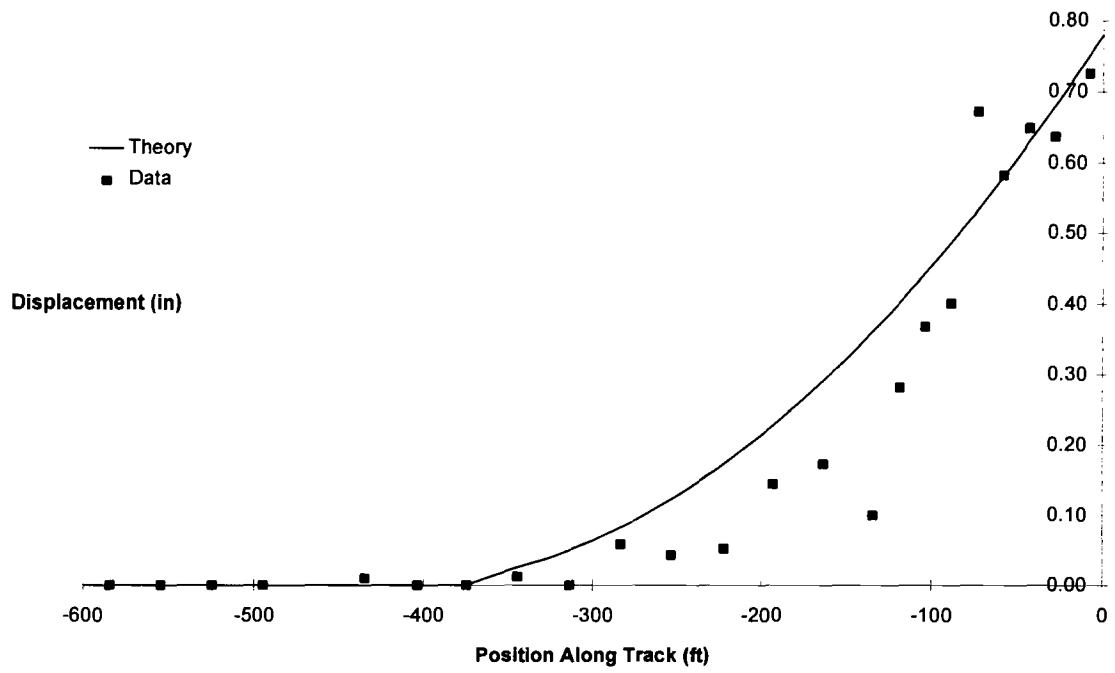


Figure 4-11. SRD5a Rail Displacement Due to Cut

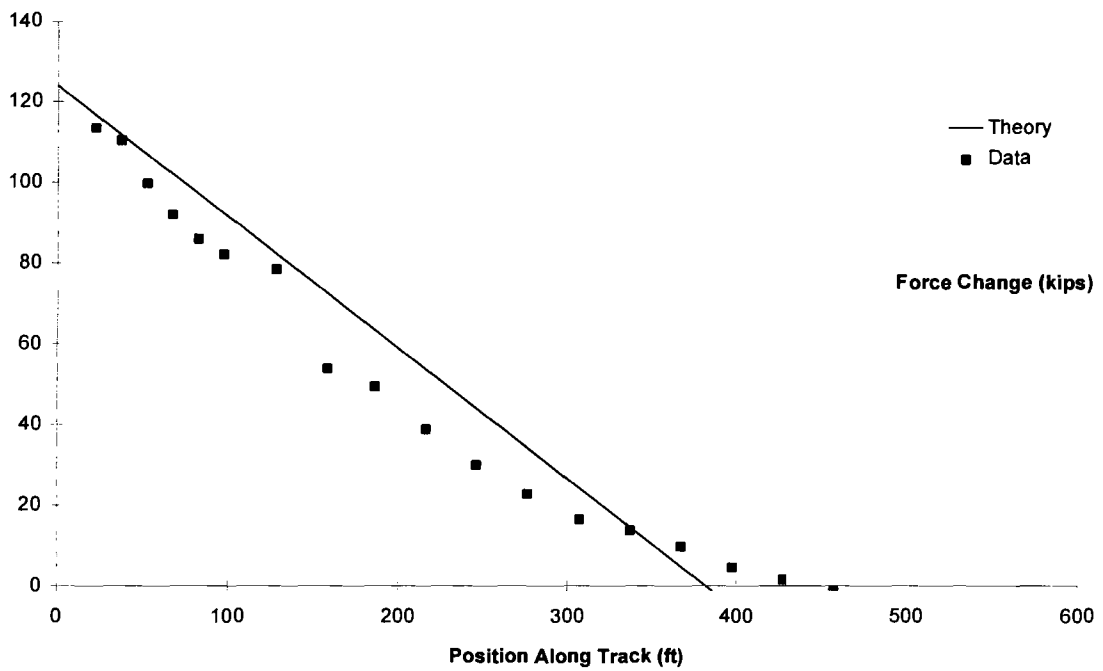


Figure 4-12. SRD5b Rail Force Change Due to Cut

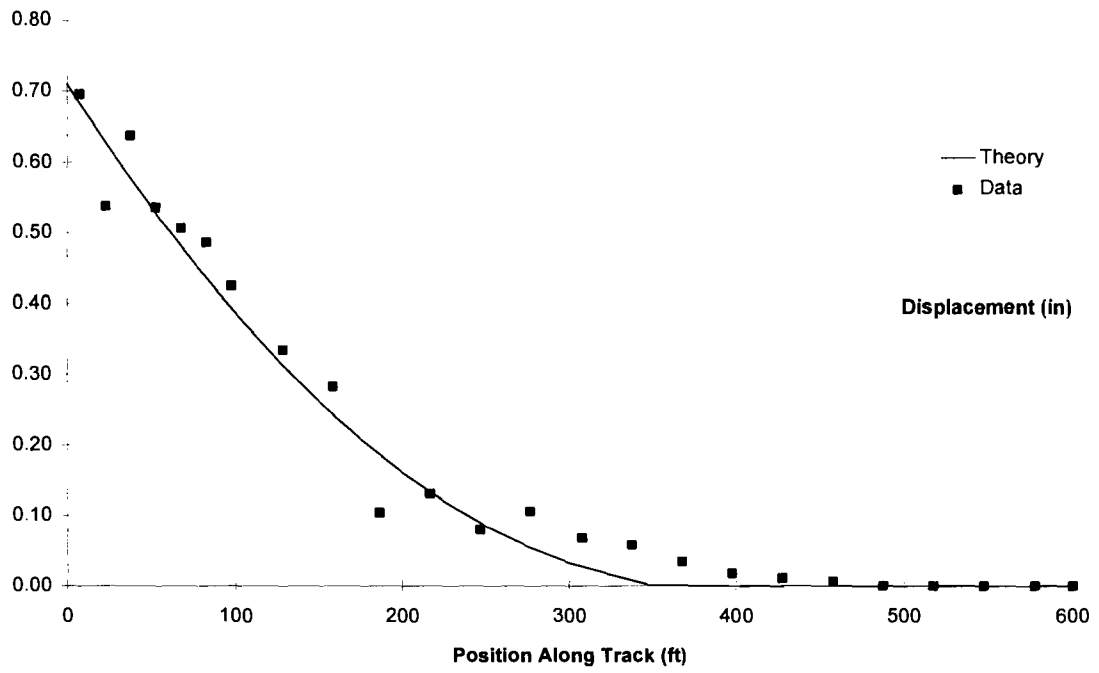


Figure 4-13. SRD5b Rail Displacement Due to Cut

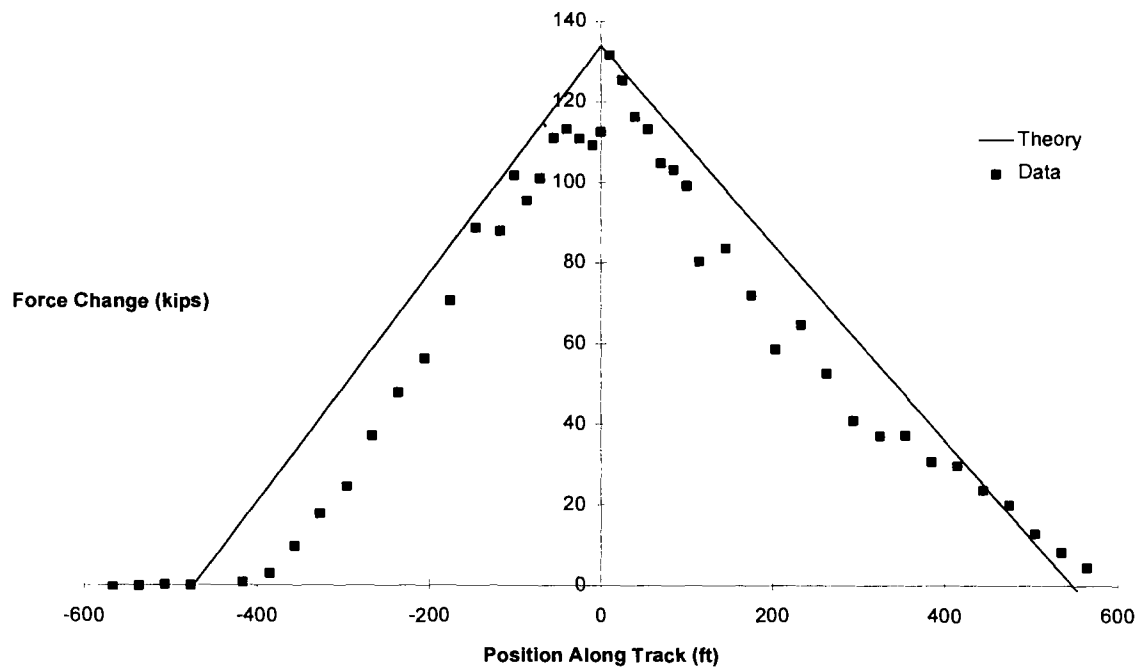


Figure 4-14. SRD6 Rail Force Change Due to Cut

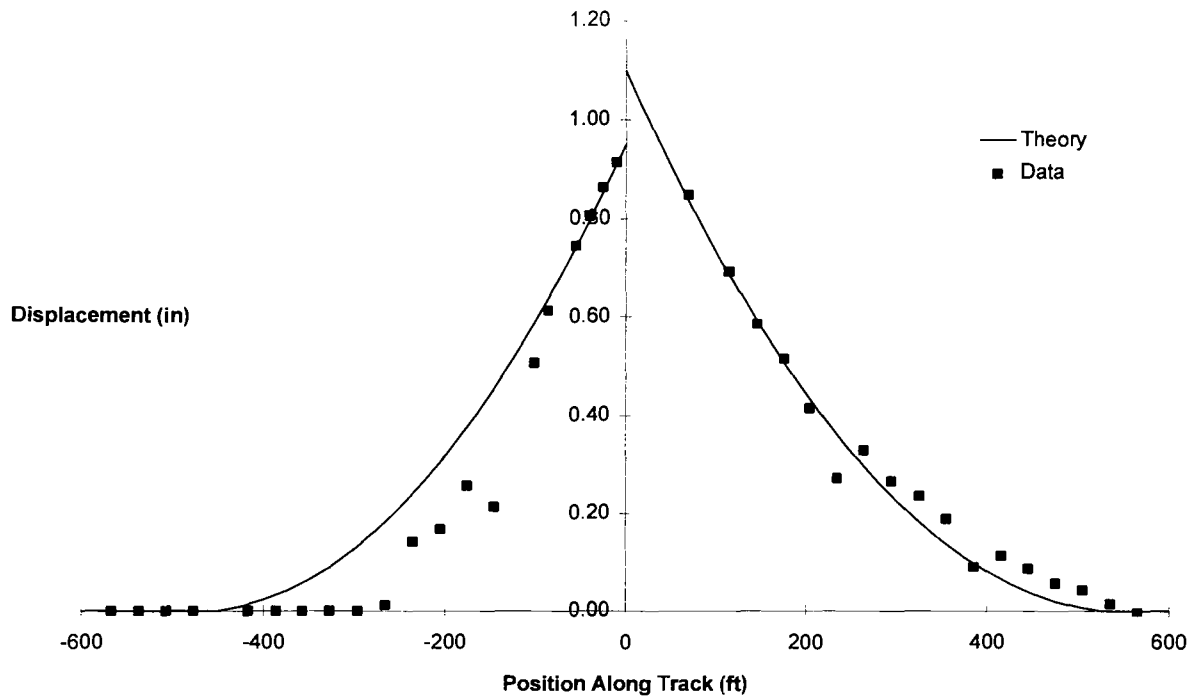


Figure 4-15. SRD6 Rail Displacement Due to Cut

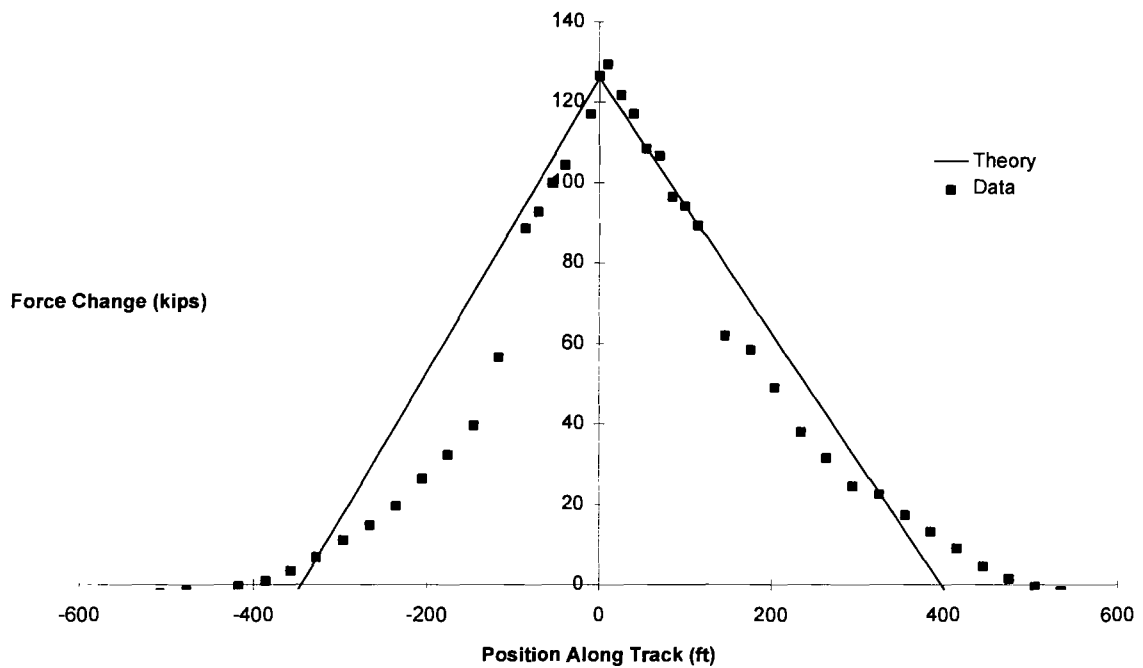


Figure 4-16. SRD7 Rail Force Change Due to Cut

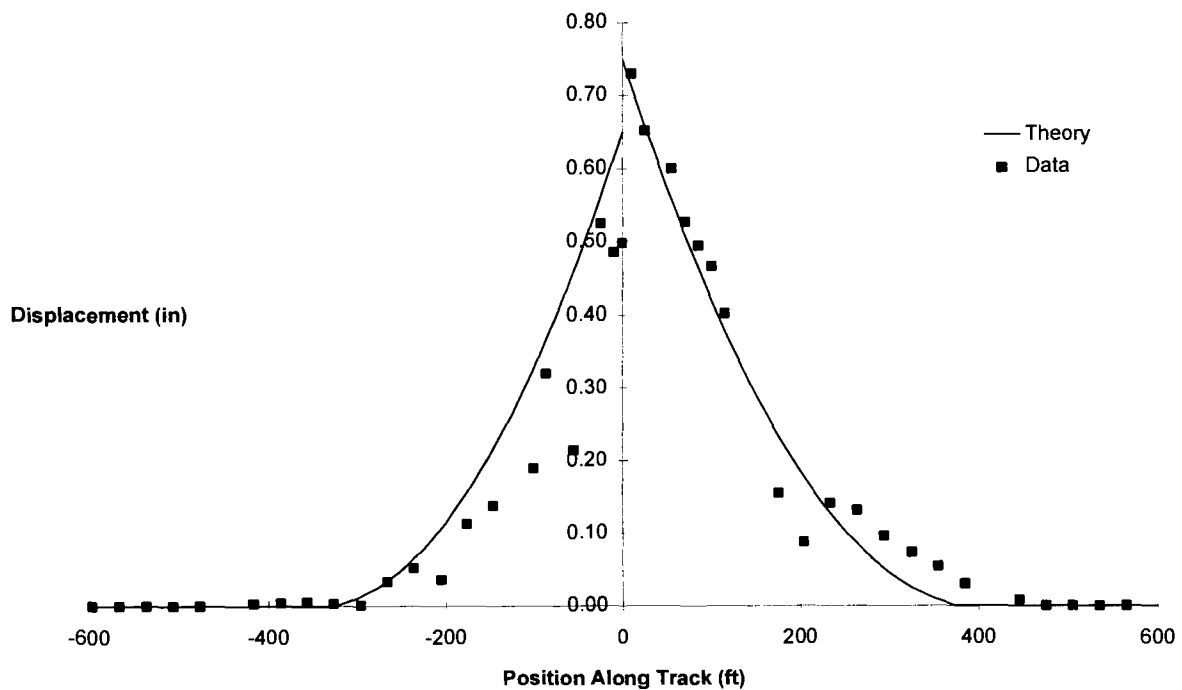


Figure 4-17. SRD7 Rail Displacement Due to Cut

Correlation with Force and Displacement Fields

Detailed test and theoretical correlations on force change and displacement fields are presented in Figures 4-2 to 4-17. The correlations are considered to be reasonable, considering nonuniform track conditions and nonuniform rail force in some of the tests.

4.3.3 Key Findings

1. The proposed theory based on constant longitudinal resistance idealization appears to be reasonable for predictions of the rail longitudinal response under summer CWR destressing operations.
2. As in Winter Rail Break simulations, the tests on Summer Destressing operations indicate that rail longitudinal resistance depends on the anchoring pattern of the test rail. The test data on the resistances is almost equal to the data previously quoted for Winter Rail Break simulations. The anchoring pattern of the other rail will influence the response of the test rail.
3. The required section length can be determined from the initial rail force levels and the displacements at the cut location. Within the assumptions made (constant longitudinal resistance and linear initial force distribution), it is not necessary to know the initial force distribution for the calculation of deanchored section. The latter is significantly influenced by the initial force distribution.

4. In revenue service conditions, sometimes the initial force levels can be constant over much larger distances, compared to those simulated in the tests. The expected displacements in such situations are much higher than those measured in the tests. This will necessitate a greater amount of steel removal than that exercised in the tests. To illustrate this consider the SRD1 test as an example. For the longitudinal resistances derived in this test (23 lb/in. for the left and 20 lb/in. for the right), the displacements would have been about 0.9 in. on the left and 1.0 in. on the right side, if the initial force remained constant. The experimental values are 0.64 in. and 0.55 in. for the left and right sides, respectively. Note that λ , the negative slope of the initial force distribution, is different for the two halves. Consequently, to obtain the same gap of 2.26 in. as in this test, the required steel removal would be 4.16 in. for constant force condition, in comparison to 3.45 in. in the test. The amount of steel to be removed would increase significantly at higher initial force levels (≈ 200 kips) compared to the test values, since the tests simulated only about half of the peak force levels that are possible in the revenue service.

5. IMPROVED GUIDELINES FOR RAIL DESTRESSING

Certain improvements in the current guidelines followed by the railroads can be proposed on the basis of the investigations presented in the previous sections. CWR destressing and restressing typically involve:

1. Selection of a deanchored length ($2L_d$) after the rail cut for destressing.
2. Setting up the required expansion gap at a known rail temperature (T_R) to obtain the desired neutral temperature when the gap is closed.
3. Reducing the gap by rail heating or hydraulic tensioning followed by welding.

These issues will be discussed in the following paragraphs.

5.1 SELECTION OF DEANCHORED SECTION LENGTH

As stated in Section 1, it is a practice in the rail industry to cut rails to relieve excessive rail force in summer. The initial rail force is seldom uniform and may not be symmetric about the cut location. Therefore, it is desirable to determine the rail longitudinal displacements at the cut location for both halves of the cut rail. This can be accomplished by using a standard ruler, reference marks on the rail and an external reference. A simple piece of hardware can be easily developed to facilitate the measurement of the two displacements (u_1 and u_2).

The initial rail force, P_0 , at the cut location can be determined using a strain gauge. The required deanchored section lengths can be calculated using the formulae

$$L_{d1} = \frac{2u_1AE}{P_0} \quad (5-1.1)$$

$$L_{d2} = \frac{2u_2AE}{P_0} \quad (5-1.2)$$

After removing the anchors over these distances, it is desirable to vibrate or shake the deanchored rail sections with a hammer to free any locked up forces due to tie plate friction.

If rail fractures occur in winter, a temporary joint bar may be installed, or if possible rewelding may be performed without requiring removal of anchors over long sections. However, proper destressing through removal of anchors should be performed in spring time after cutting rail, if previously welded, or removing the joint bar. The CWR should be restressed to its correct neutral temperature by using the procedures in the following sections.

The procedure presented here provides rational guidelines compared to the current practice of a wide range of deanchored section lengths (200 ft to 1400 ft).

5.2 GAP ADJUSTMENT FOR RESTRESSING UNDER RAIL HEATING

In Summer Destressing, the rail temperature is usually above the desired neutral temperature (> 100°F). After rail cutting and deanchoring, the required gap is simply that for welding (≈ 1 in.) which can be obtained by an additional amount of steel removed or through insertion of a plug as per existing railroad practice. The rails can be welded immediately at the desired high neutral temperature.

If after cutting the rail, the rail temperature is allowed to drop below the desired neutral temperature (or if the rail temperature happens to be low as in the Winter Rail Break scenario) rail heating is an option for raising the rail temperature prior to rewelding. Rail heating can be done artificially (using propane gas heaters) or naturally using the solar energy when possible. The required gap at the neutral temperature, $T_R (< T_N)$ depends on the type of heating.

5.2.1 Artificial Heating

It will be assumed that the artificial heating is confined to the deanchored rail sections. If the deanchored length on either side is L_d , the gap is

$$\Delta = \delta + 2\alpha L_d \Delta T \quad (5-2)$$

where the second term on the right hand side represents the free thermal expansion of the deanchored sections, and

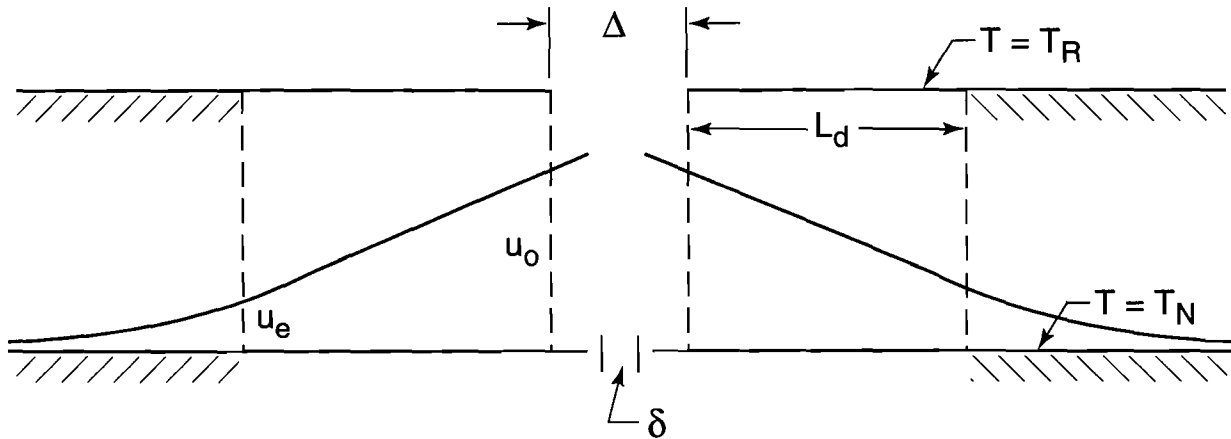
$$\begin{aligned} \delta &= \text{Welding allowance } (\approx 1 \text{ in.}) \\ T_N &= \text{Neutral temperature} \\ T_R &= \text{Rail temperature} \\ \Delta T &= T_N - T_R \end{aligned}$$

5.2.2 Solar Heating

If solar heating is used, one must remember that not only the deanchored sections but the anchored rail beyond will be heated. The constrained expansion of the anchored section should also be accounted for in the adjustment of the gap (see Figure 5-1).

$$\Delta = \delta + 2\alpha L_d \Delta T + 2u_e \quad (5-3)$$

where u_e is the movement of the rail at the transition point between the anchored and unanchored regions. The second term on the right represents the free expansion of the unanchored rail section. It can be shown that



320-DTS-95190-46

Figure 5-1. End Movement in Solar Heating Method of Restressing

$$u_e = \frac{AE(\alpha\Delta T)^2}{2f_0} \quad (5-4)$$

and

$$\Delta - \delta = 2\alpha L_d \Delta T \left\{ 1 + \frac{AE\alpha\Delta T}{2f_0 L_d} \right\} \quad (5-5)$$

The last term is the correction factor due to the movement of the anchored semi-infinite track sections on either side. For weak track (low longitudinal resistance) and large differential between the desired neutral temperature and the rail temperature at which the gap is adjusted, the contribution from the last term can be significant.

Example: Consider a rail at 40°F, deanchored over 325 ft on both sides. Determine the gap required to obtain an installed rail neutral temperature of 100°F. Assume that the rail longitudinal resistance = 20 lb/in.

$$\begin{aligned} \text{Free "thermal" expansion} &= 2L_d\alpha\Delta T \\ &= 2(12)(325)(6.4 \times 10^{-6})(100 - 40) \\ &= 3 \text{ in.} \end{aligned}$$

$$\begin{aligned}
\text{Correction Factor} &= 1 + \frac{AE\alpha\Delta T}{2f_0L_0} \\
&= 1 + \frac{(13.35)(30 \times 10^6)(6.4 \times 10^{-6})(100 - 40)}{2(20)(325)(12)} \\
&= 1.99
\end{aligned}$$

$$\begin{aligned}
\text{Required Gap} &= 3(1.99) + \delta \text{ (welding allowance)} \\
&= 5.95 + \delta \text{ (in.)}
\end{aligned}$$

If no correction is employed, effective ΔT for 3 + δ in. gap is

$$\begin{aligned}
\Delta T_{\text{eff}} &= \frac{60}{5.95} (3) \\
&= 30.2^\circ\text{F}
\end{aligned}$$

Hence, resulting T_N with no correction for end movement

$$\begin{aligned}
&= 40 + 30.2 \\
&= 70.2^\circ\text{F}
\end{aligned}$$

instead of the intended T_N of 100°F.

5.3 GAP ADJUSTMENT UNDER HYDRAULIC TENSIONING

The expansion gap stipulated by the railroads for hydraulic tensioning is based on the free expansion of the deanchored rail section. This method by which the expansion gap is closed for rewelding needs to be assessed properly. Although the hydraulic expander method was not studied in the tests described in this report, the test data generated here from the solar heating of the entire track (anchored and deanchored sections) revealed that there would be some longitudinal movement even in the anchored section, particularly at the common point between the anchored and deanchored zones. This "end movement" of the deanchored rail section must be accounted for to obtain an accurate estimate of the expansion gap required prior to welding in order to yield the desired neutral temperature. Figure 5-2 illustrates the correction required while using the hydraulic expander. Under the mechanical force \bar{p} , the initial gap, Δ , will be reduced to δ . It can be shown that:

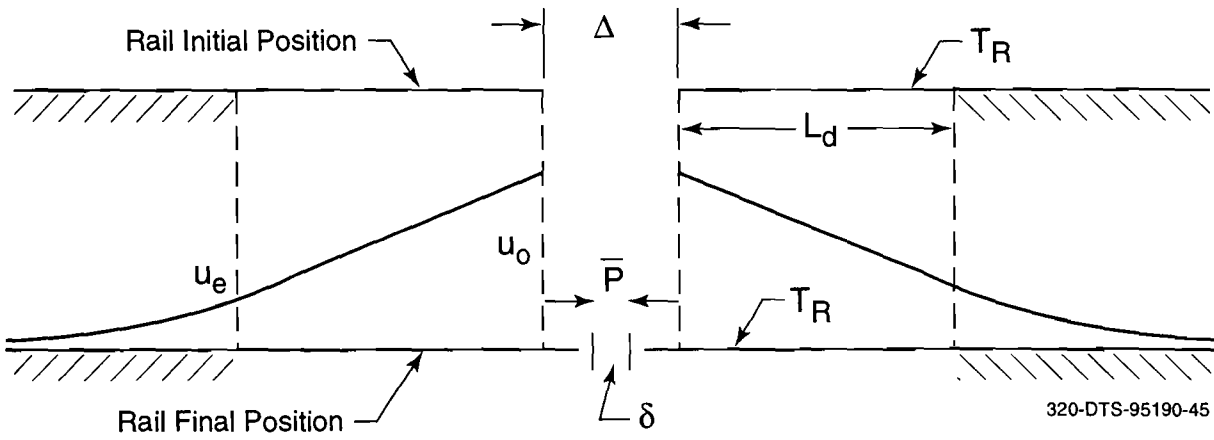


Figure 5-2. End Movement in Hydraulic Expander Method of Restressing

$$\Delta = \delta + \frac{2\bar{P}L_d}{AE} + 2u_e \quad (5-6)$$

where

$$\begin{aligned} \bar{P} &= \text{Equivalent mechanical force corresponding to } \Delta T = T_N - T_R \\ &= AE\alpha(T_N - T_R) \end{aligned}$$

u_e = End movement of anchored rail as previously defined

Neglecting the friction drop from the center to the end of the deanchored rail section (ideally, the rail should be vibrated or kept on rollers), one finds that

$$u_e = \frac{\bar{P}^2}{2AEf_0} \quad (5-7)$$

Hence,

$$\Delta - \delta = 2L_d\alpha\Delta T + \frac{AE(\alpha\Delta T)^2}{f_0} \quad (5-8)$$

$$\Delta - \delta = 2L_d\alpha\Delta T \left\{ 1 + \frac{AE\alpha\Delta T}{2f_0L_d} \right\}$$

The term in the brackets represents the required correction factor for the expansion gap that is in current usage by the industry. This expression is similar to that derived previously in subsection 5.2.2. Hence, for the same example as in subsection 5.2.2, a loss of $29.8^{\circ}F$ loss of the intended T_N of $100^{\circ}F$ is anticipated, if no correction is applied.

6. CONCLUSIONS AND RECOMMENDATIONS

6.1 CONCLUSIONS

1. The longitudinal rail force and displacement distribution in the cut rail are governed by the rail longitudinal resistance and the initial rail force level prior to cut. The resulting gaps from Winter Rail Break and rail movement under summer cut for excessive rail removal will also depend on these two parameters. Analysis and test correlations have shown that by measuring the rail displacements and the initial force distribution, the longitudinal resistance can be evaluated.
2. The longitudinal resistance of the ETA track is about twice the value for EOTA. For the wood tie track with cut spike construction tested at TTC, Pueblo, CO, the resistance for the EOTA track is about 17 lb/in.
3. From the rail force and the displacements at the cut location, one can determine the required deanchored length for destressing the rail within a limit (say, 20 kips). The required deanchored length depends on the initial force and the longitudinal resistance. Determination of the optimum required deanchored length is important as an underestimated value can lead to an incorrect setting of the neutral temperature.
4. The required deanchored section length for rail destressing is not only dependent on the absolute initial force at the cut location but also on the force distribution. If the force can be idealized as varying linearly, the negative slope of this linear distribution, λ , has a significant influence on the longitudinal response of the cut rail. If the force is uniform ($\lambda = 0$), the required deanchored section length for EOTA is twice that of ETA, when all other conditions (initial force, P_0 , type of anchors, ballast, etc.) are the same. For the track tested at TTC, required deanchored lengths were found to be in the range of 300 ft to 600 ft on either side of the cut, depending on the initial rail force level and its distribution. The theory indicates that higher deanchored lengths would have been required, if the initial force was uniform and did not fall off from the cut location.

Rail gap on the order of 3.5 in. was measured in Winter Rail Break simulations at a rail force of about 190 kips. According to the theory, a gap of about 5.6 in. can be anticipated under the same track conditions, if the initial force were uniform.

5. When restressing is performed under solar heating or using the hydraulic tensioning of the deanchored zone, care must be taken to increase the initial “expansion gap” accounting for the rail longitudinal movement in the anchored zone, in addition to the welding allowance. The movement in the anchored zone was observed in the tests under solar heating. Although no tests were performed using the hydraulic tensioning, significant end movement is predicted on the basis of theoretical and test investigations presented in this report. Required expansion gap formulae are presented in this report on the basis of the rail longitudinal resistance due to anchors. If the current railroad procedures are used for the expansion gap

under hydraulic tension, significant errors in the neutral temperature can occur depending upon the desired neutral temperature differential and the longitudinal resistance.

6.2 RECOMMENDATIONS

1. Tests on revenue service track are desirable to estimate the longitudinal resistance found on typical tracks. If the longitudinal resistance can be quantified reliably for revenue tracks (by using the rail cutting method used in this report), then there may not be any need to measure the rail force, since all the required information can be expressed in terms of the resistance and the measured gap at rail cut locations.
2. The proposed improved guidelines in destressing and expansion gap adjustment should be validated by tests on commercially available hydraulic tensioning devices. This is particularly important as the rail industry is increasing the usage of such devices in CWR restressing, which under the current practice can result in lower nonconservative neutral temperatures.

APPENDIX - INITIAL RAIL FORCE DISTRIBUTIONS - LINEAR FITS

The test data on the rail force distribution is shown in the following figures. A linear regression line has been fitted for the data.

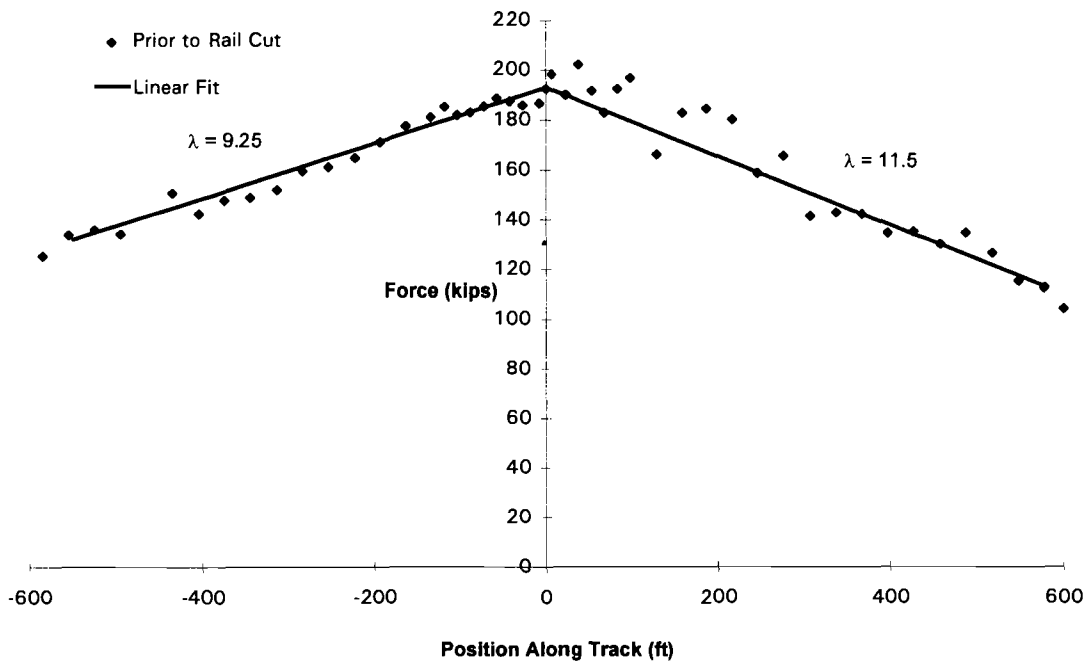


Figure A-1. WRB1 Initial Rail Force

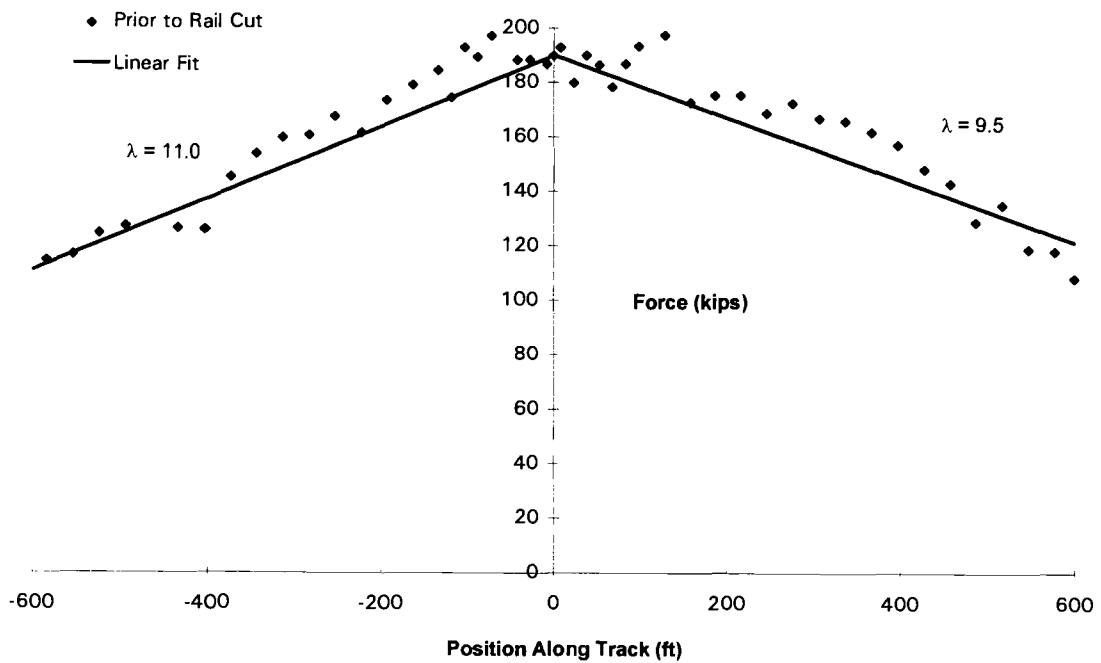


Figure A-2. WRB2 Initial Rail Force

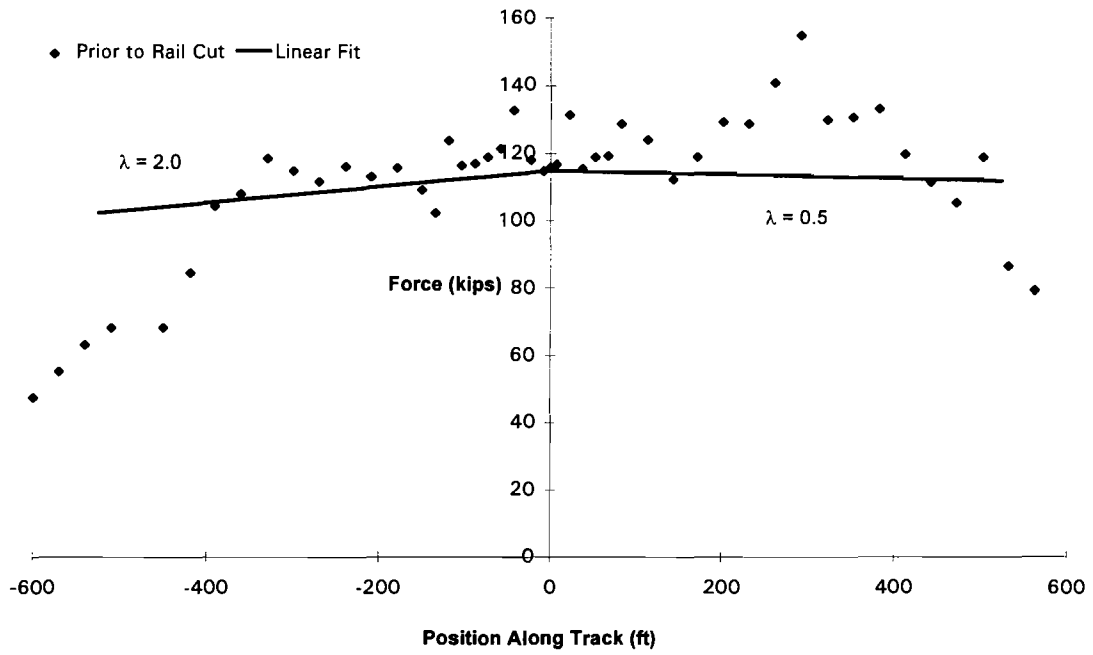


Figure A-3. WRB3 Initial Rail Force

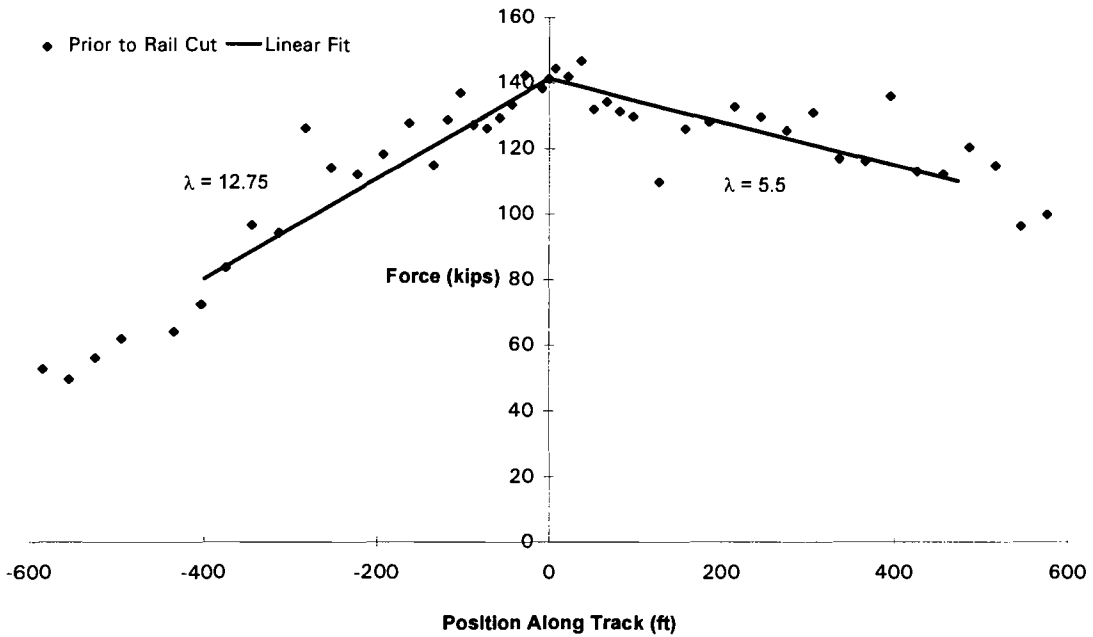


Figure A-4. WRB4 Initial Rail Force

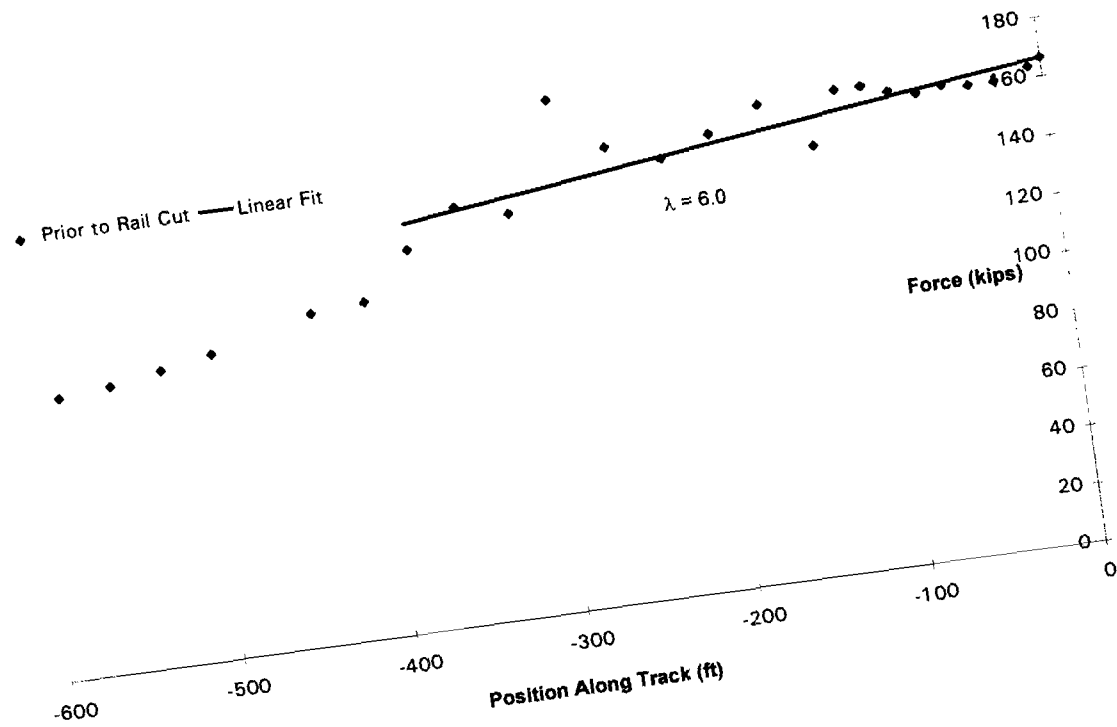


Figure A-5. WRB5a Initial Rail Force

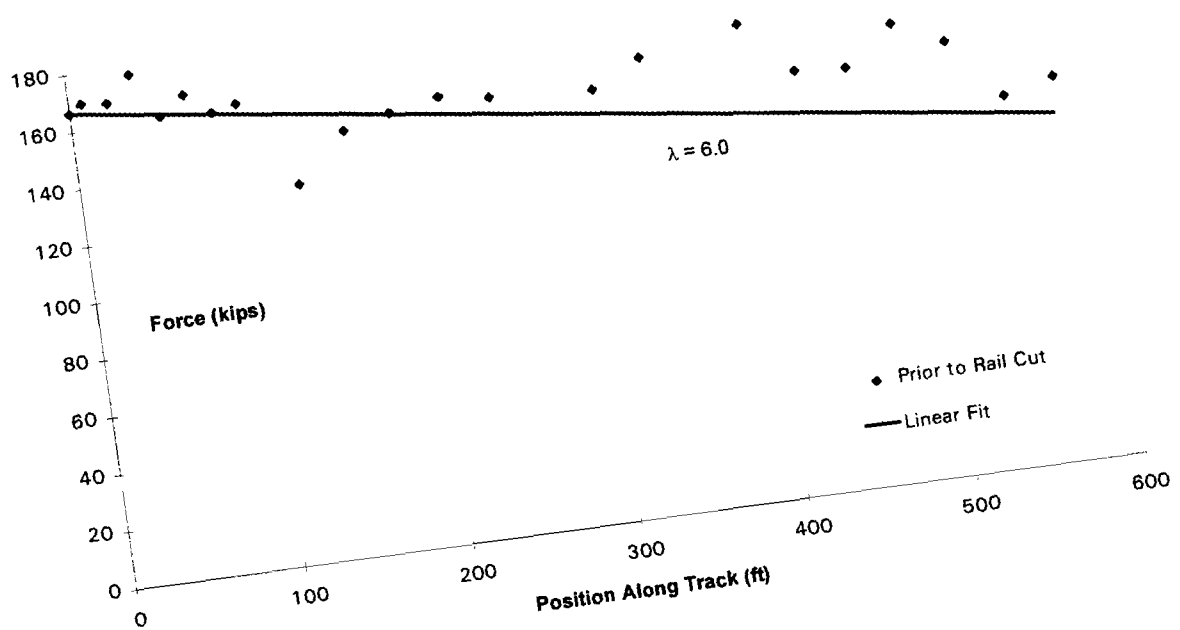


Figure A-6. WRB5b Initial Rail Force

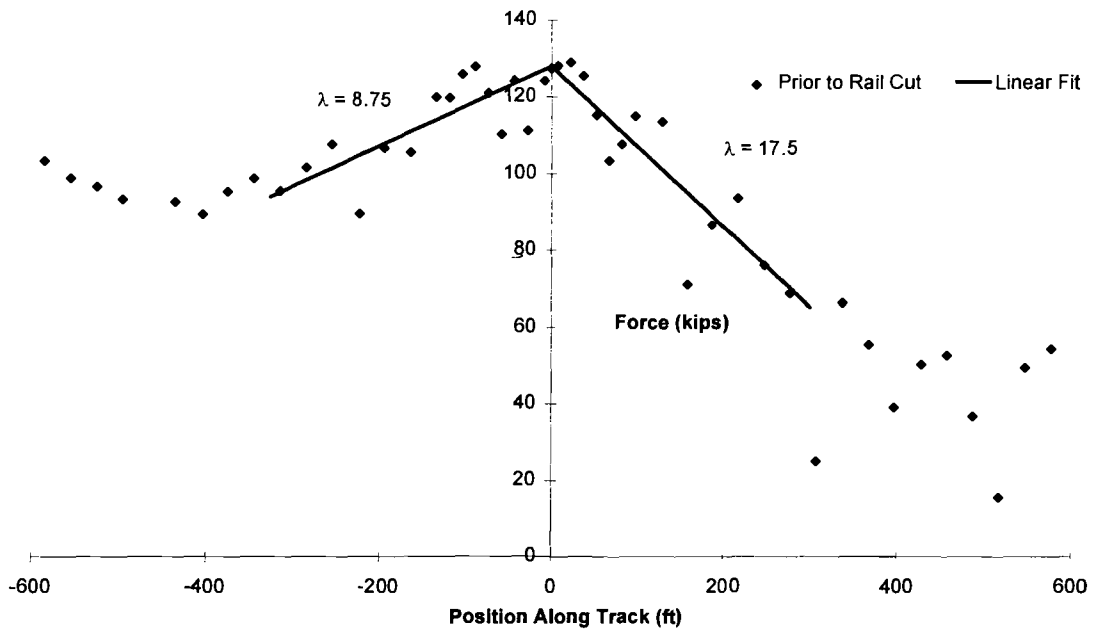


Figure A-7. SRD1 Initial Rail Force

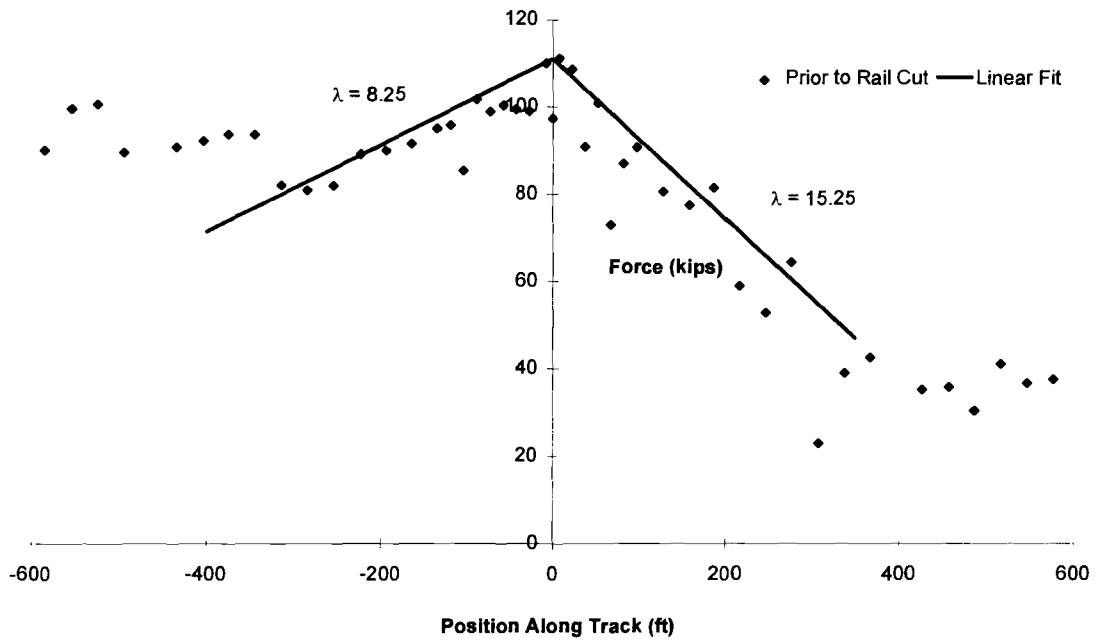


Figure A-8. SRD2 Initial Rail Force

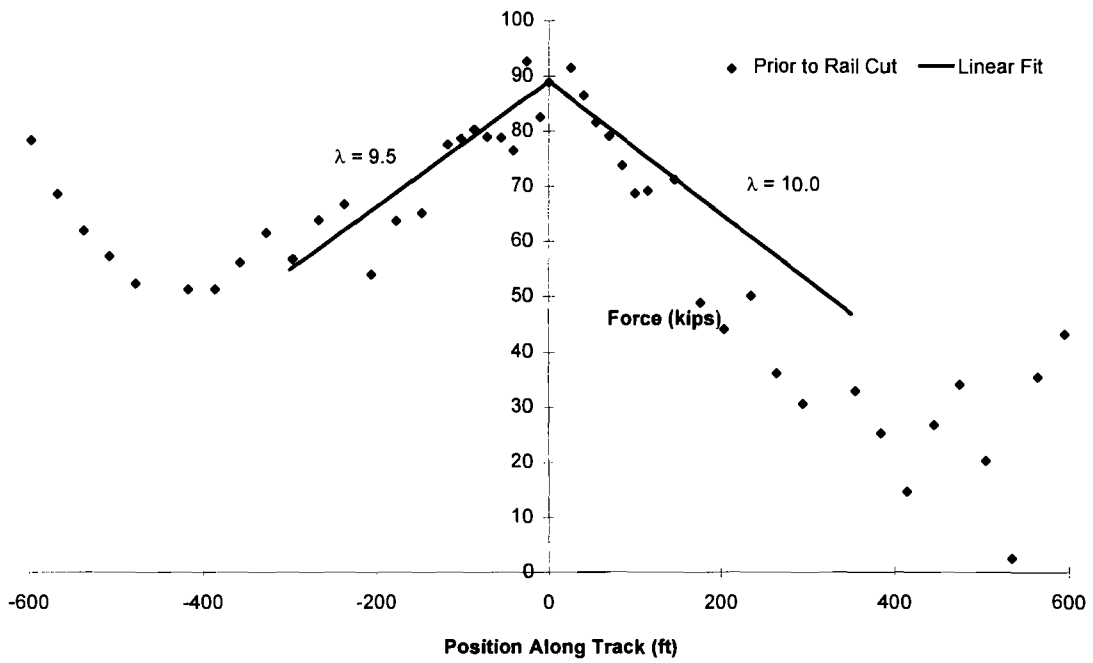


Figure A-9. SRD3 Initial Rail Force

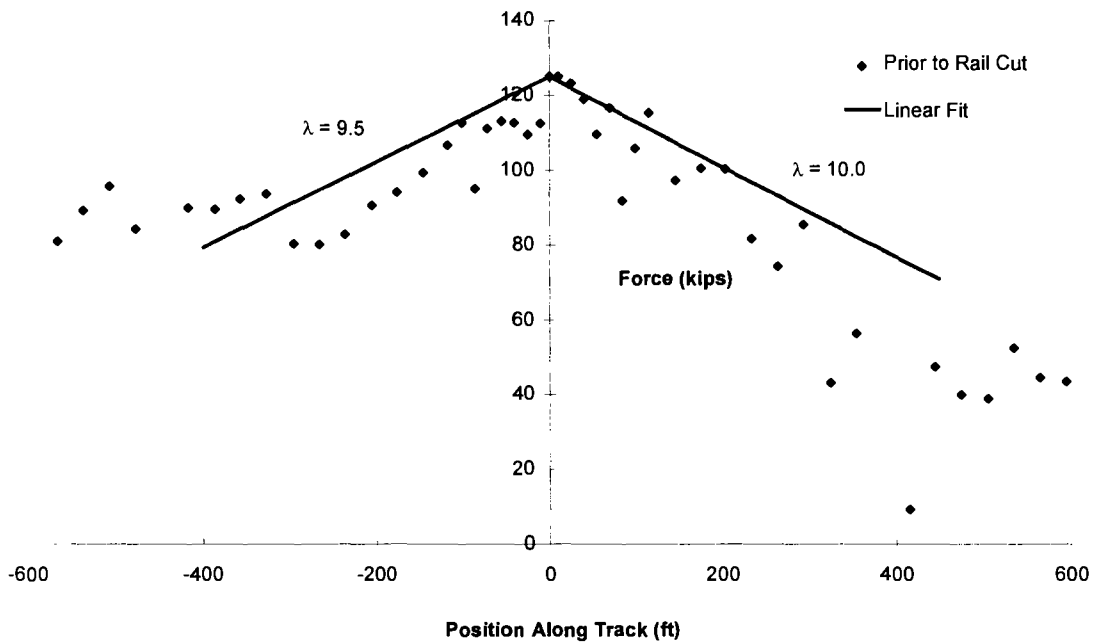


Figure A-10. SRD4 Initial Rail Force

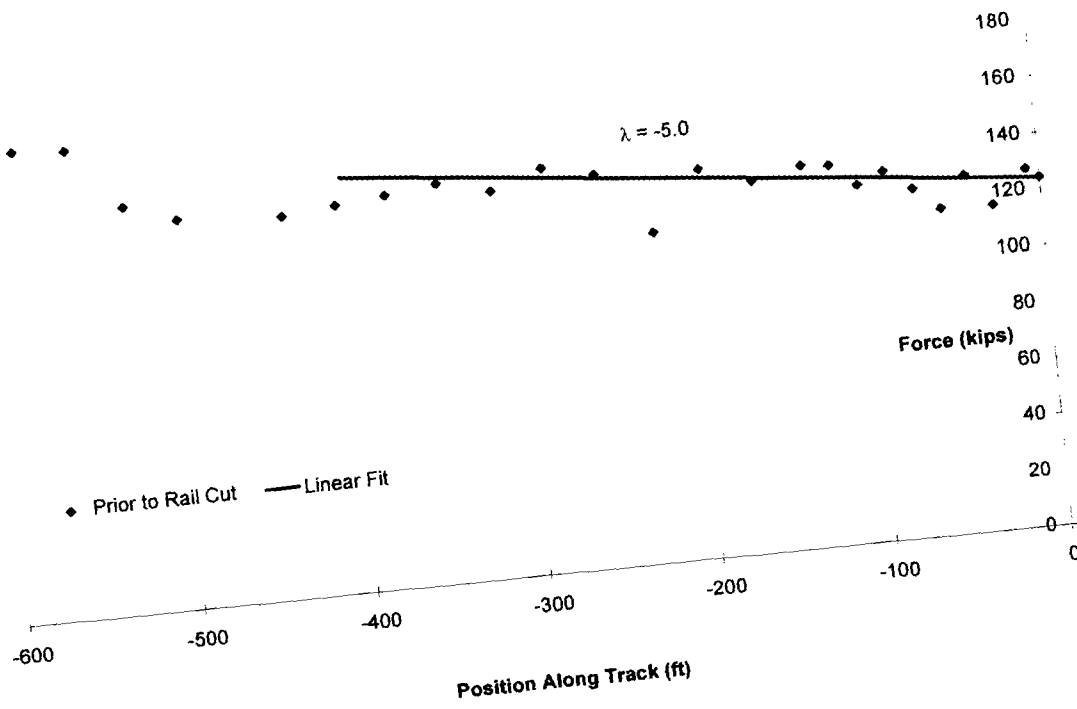


Figure A-11. SRD 5a Initial Rail Force

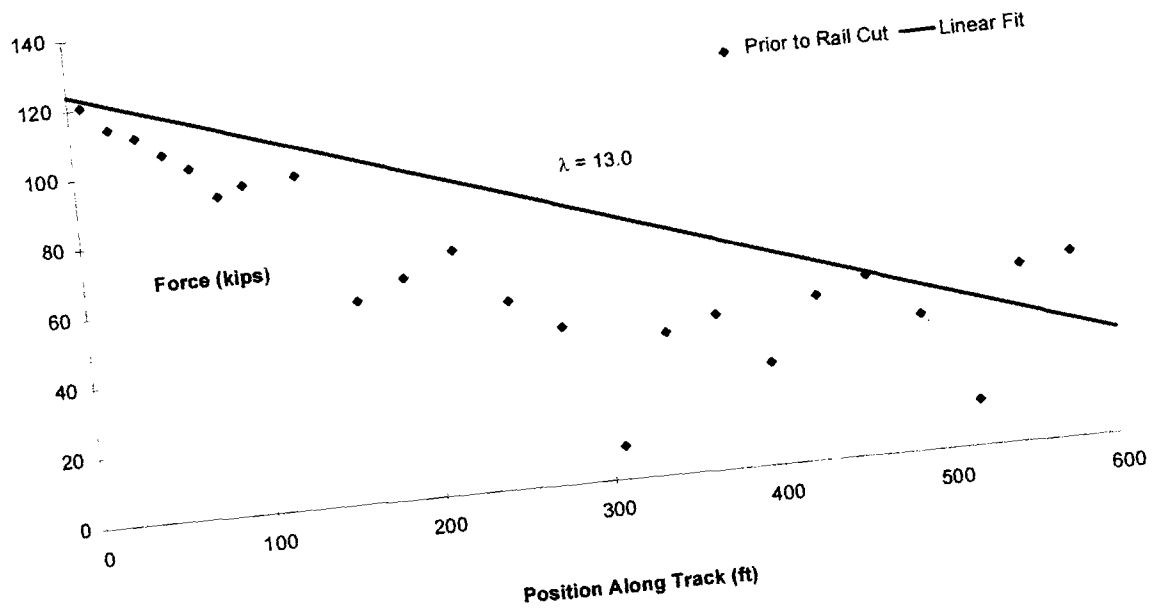


Figure A-12. SRD 5b Initial Rail Force

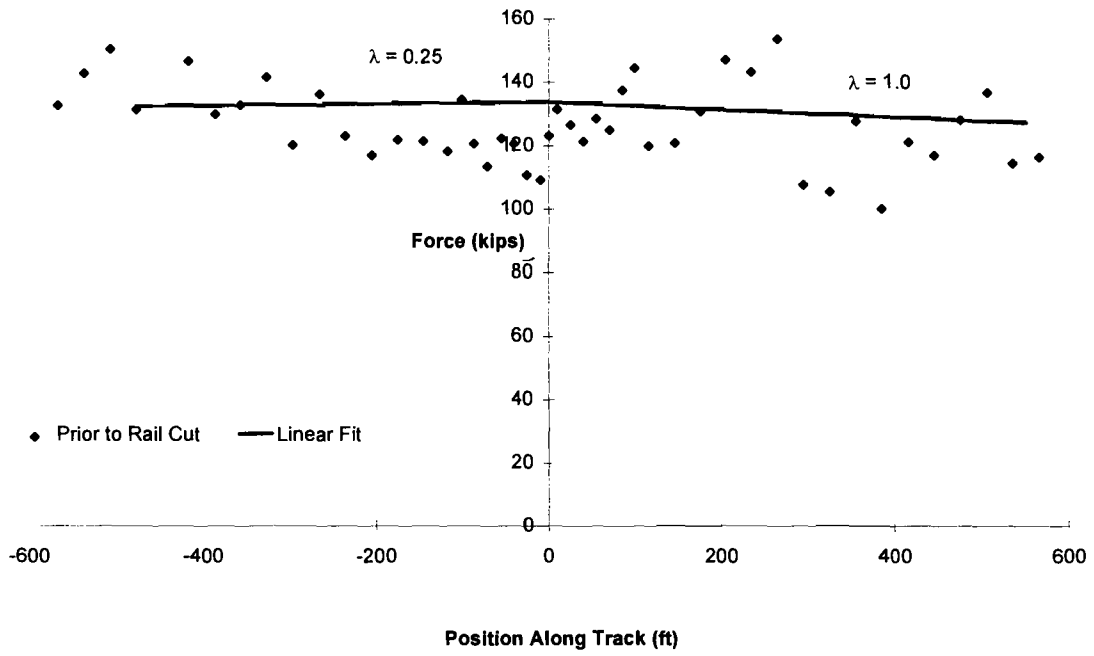


Figure A-13. SRD 6 Initial Rail Force

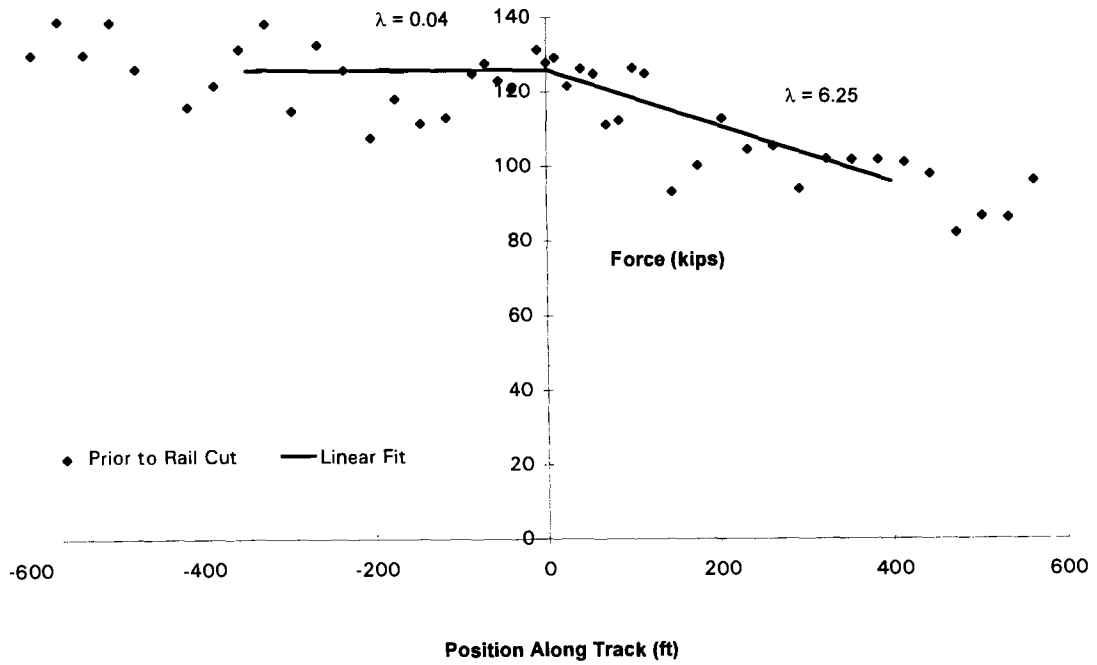


Figure A-14. SRD7 Initial Rail Force

REFERENCES

1. Samavedam, G., Kish, A., Purple, A. and J. Schoengart, "Parametric Analysis and Safety Concepts of CWR Track Buckling," DOT/FRA/ORD-93/26, DOT-VNTSC-FRA-93-25, Final Report, December 1993.
2. Samavedam, G. and A. Purple, "The Influence of Rail Anchors/Fasteners on Rail Breaks and Destressing," Technical Note prepared for U.S. DOT, Volpe Center, 1993.



